A novel small molecular weight compound with a carbazole structure that demonstrates potent human immunodeficiency virus type-1 integrase inhibitory activity

Hua Yan[1], Tomoko Chiba Mizutani[1], Nobuhiko Nomura[2], Tadakazu Takakura[2], Yoshihiro Kitamura[3], Hideka Miura[1], Masako Nishizawa[1], Masashi Tatsumi[1], Naoki Yamamoto[1] and Wataru Sugiura[1*]

[1]AIDS Research Center, National Institute of Infectious Diseases, Tokyo, Japan
[2]Research and Discovery Laboratories, Toyama Chemical Co. Ltd., Toyama, Japan
[3]Division of Infectious Diseases, Advanced Clinical Research Center, Institute of Medical Science, University of Tokyo, Japan.

*Corresponding author: Tel: +81 42 561 0771; Fax: +81 42 561 7746; E-mail: wsugiura@nih.go.jp

The integration of reverse transcribed proviral DNA into a host genome is an essential event in the human immunodeficiency virus type 1 (HIV-1) replication life cycle. Therefore, the viral enzyme integrase (IN), which plays a crucial role in the integration event, has been an attractive target of anti-retroviral drugs. Several IN inhibitory compounds have been reported previously, yet none has been successful in clinical use. To find a new, more successful IN inhibitor, we screened a diverse library of 12 000 small molecular weight compounds randomly by *in vitro* strand-transfer assay. We identified a series of substituted carbazoles that exhibit strand-transfer inhibitory activity at low micromolar concentrations. Of these, the most potent compound exhibited an IC_{50} of 5.00 ±3.31 μM (CA-0). To analyse the structural determinants of strand-transfer inhibitory activity of the carbazole derivatives, we selected 23 such derivatives from our compound library and performed further analyses. Of these 23 compounds, six showed strong strand-transfer inhibition. The inhibition kinetics analyses and ethidium bromide displacement assays indicated that the carbazole derivatives are competitive inhibitors and not intercalators. An HeLa4.5/LTR-nEGFP cell line was employed to evaluate *in vitro* virus replication inhibition of the carbazole derivatives, and IC_{50} levels ranged from 0.48–1.52 μM. Thus, it is possible that carbazole derivatives, which possess structures different from previously-reported IN inhibitors, may become novel lead compounds in the development of IN inhibitors.

Keywords: integrase inhibitor, carbazole, HIV-1, antiretroviral drug

Introduction

Human immunodeficiency virus type 1 (HIV-1), causative agent of acquired immunodeficiency syndrome (AIDS), possesses three critical enzymes for replication. These are protease (PR), reverse transcriptase (RT), and integrase (IN) (Ruscetti, 1985; Kohl *et al.*, 1988; LaFemina *et al.*, 1992). As inactivating any of these enzymes may negate the infectivity of HIV-1, the enzymes have been targets of anti-retroviral drug development. Indeed, great progress in anti-retroviral drug discovery has been achieved in recent decades, and today 10 RT inhibitors and eight PR inhibitors (De Clercq, 1992; Tronchet & Seman, 2003; Balzarini, 2004; Imamichi, 2004) are available for anti-retroviral treatments. The third enzyme, IN, has also been a major target of inhibitor development. L-708,906 and L-731,988, which possess diketo acid moieties within their structures, were the first IN-specific inhibitors discovered (Pommier *et al.*, 2000; Dayam & Neamati, 2003; Pluymers *et al.*, 2002; Hazuda *et al.*, 2000). S-1360 and L-870,810, which also have diketo acid moieties, are IN inhibitors that have reached clinical Phase I/II trials for the first time (Johnson *et al.*, 2004; Hazuda *et al.*, 2004). However, although there have been large advances in the development of IN inhibitors, further research and analysis is required to develop clinically usable compounds.

Integrase (IN), the leading target of novel anti-retroviral inhibitor development, is the enzyme responsible for integration, wherein reverse transcribed HIV-DNA is inserted into a host genome, and is critical for viral replication, which in turn establishes latency and chronic infection (Chun *et al.*, 1995). IN is composed of three distinct

domains – the N-terminal domain (amino acids 1–50) with a zinc-binding motif (Schauer & Billich, 1992; Burke *et al.*, 1992), the catalytic core domain (amino acids 50–212) with polynucleotidyl transfer activity and sequence-specific endonuclease activity (Engelman & Craigie, 1992; Engelman *et al.*, 1994) and the C-terminal domain (amino acids 212–288), which has been thought to relate to nonspecific DNA binding (Khan *et al.*, 1991; Woerner & Marcus-Sekura, 1993).

At present, the function and structure of each domain has not been fully understood. The most well-analysed domain is the catalytic core domain, and its active site has highly conserved amino acidic residues Asp64, Asp116 and Glu152, which are critical for polynucleotidyl transfer activity (LaFemina *et al.*, 1992; Engelman *et al.*, 1995). Previously reported potent IN inhibitors L-708,906, L-731,988, L-801,810, S-1360 and 5-CITEP are all targeted to this domain. These inhibitors bind to the active site, displace divalent metal ion Mg^{2+} from the active site and inactivate the catalytic activity of IN (Grobler *et al.*, 2002; Dayam & Neamati, 2003; Goldgur *et al.*, 1999; Johnson *et al.*, 2004). No specific inhibitors have been reported for the N-terminal and C-terminal domains.

In the present study we attempted to identify novel IN inhibitory compounds, and therefore we conducted a random screening of a library of small molecular weight compounds. As a result, we discovered a series of novel IN inhibitory compounds with carbazole structures, that are quite different from previously reported inhibitory compounds.

Materials and methods

Preparation of integrase

The sequence coding the NL4-3 integrase (IN) was cloned into pET28b(+) (Novagen, Madison, WI, USA), generating pET-IN that codes NL4-3 IN with a hexa-histidine tag at the N-terminus. *Escherichia coli* strain Rosetta (DE3) (Novagen) transformed with pET-IN was grown in 1 l of Super Broth (Biofluids, Camarillo, CA, USA) containing 100 μg/ml kanamycin at 30°C until the optical density of the culture had reached between 0.5 and 0.7 at 600 nm. The recombinant protein expression was induced by isopropyl-1-thio-D-galactopyranoside. After incubation for 3 h, the cells were harvested and resuspended in 100 ml of preparation buffer (20 mM Tris-HCl, pH 8.0, 0.5 M NaCl) and disrupted by sonication. Following high-speed centrifugation at 40 000×g for 45 min at 4°C, the pellet was homogenized in GBB buffer (50 mM Tris-HCl, pH 8.0, 6 M Guanidine HCl and 2 mM 2-ME). The residual pellet was again sonicated and centrifuged at 40 000×g for 30 min at 4°C.

The supernatant was filtered through a 0.22 μm filter and mixed with 1 ml of nickel-affinity resin (Sigma, St. Louis, MO, USA), and incubated overnight at 4°C. The resin was washed twice by mixing with 20 ml of GBB containing 5 mM imidazole (Sigma). The protein was eluted with GBB containing 1 M imidazole. The fractions containing integrase were pooled and 0.5 M EDTA was added to a final concentration of 5 mM. This eluted protein was then sequentially dialysed against (i) 6 M guanidine HCl, 50 mM Tris-HCl (pH 8.0), 2 mM 2-ME, 1 mM EDTA for 2 h at room temperature, (ii) 6 M guanidine HCl, 50 mM Tris-HCl (pH 8.0), 10 mM DTT, 1 mM EDTA for 16 h at room temperature, (iii) 4 M urea, 50 mM Tris-HCl (pH 8.0), 0.5 M NaCl, 1 mM DTT, 0.1 mM EDTA for 16 h at 4°C, (iv) 2 M urea, 50 mM Tris-HCl (pH 8.0), 0.5 M NaCl, 1 mM DTT, 0.1 mM EDTA, 20% (w/v) glycerol for 16 h at 4°C, (v) 1 M urea, 50 mM Tris-HCl (pH 8.0), 1 M NaCl, 1 mM DTT, 0.1 mM EDTA, 15 mM 3-[(3-cholamidopropyl) dimethylammonio]-1-propanesulfonate (CHAPS), 20% (w/v) glycerol for 16 h at 4°C, and (vi) 50 mM Tris-HCl (pH 8.0), 1 M NaCl, 1 mM DTT, 0.1 mM EDTA, 15 mM CHAPS, 20% (w/v) glycerol for 16 h at 4°C. The final preparation was stored at −80°C.

The purified enzyme activity was confirmed and evaluated by strand-transfer assay using M8 apparatus (IGEN, Gaithersburg, MD, USA).

Preparation of test compounds

A diverse library of 12 000 small-molecule compounds was supplied by Toyama Chemicals Co. Ltd. (Toyama, Japan). All test compounds were dissolved in DMSO and adjusted to 2 mM concentration. S-1360 was synthesized as positive control for strand transfer assay.

Construction of strand-transfer assay

Two different strand-transfer assay systems were employed in the IN inhibitor screening trial. For the first screening step, an M8 apparatus and strand-transfer assay kit, ORIGEN HIV integrase assay (IGEN), was used. In brief, magnetic beads coated with 29 mer donor double-stranded DNA (dsDNA) were mixed with purified IN (15 pmol), followed by adding the test compound and 20 mer target dsDNA tagged with ruthenium, conducting electronically inducible fluorescence chemistry, and incubating for 1 h at 37°C. Subsequently, the entire reaction solution was applied to the M8 apparatus, and then strand-transfer products were captured by a magnet in the flow-circuit of the equipment. The amount of the strand-transfer product was measured by ruthenium fluorescence activity. For the second and later screening steps, in-house strand-transfer assay was employed. The in-house assay was designed in 96-well plate format to achieve high-throughput screening.

The following donor and target DNA oligonucleotides were designed and used:
Donor-1 (D1): 5′-ACTGCTAGAGATTTTCCA-CACTGACTAAAAG-3′
Donor-2 (D2): Biotin-5′-CTTTTAGTCAGTGTGGA-AAATCTCTAGCA-3′
Target-1 (T1): 5′-CTAGAGATTTTCCACACTGACT-AAAAG-3′-Digoxigenin (DIG),
Target-2 (T2): 5′-CTTTTAGTCAGTGTGGAAAA-TCTCTAG-3′-DIG

To form dsDNA, the D1–D2 pair and the T1–T2 pair were mixed in the presence of 0.1 M NaCl and denatured for 10 min at 95°C, followed by an annealing process, gradual cooling down to room temperature. One pmol biotinulated donor dsDNA (D1–D2), 15 pmol IN protein and 5 µl test compounds (100 µM in DMSO) were mixed together in assay buffer (25 mM 3-(N-morpholino)-propanesulfonic acid, pH 7.2, 25 mM NaCl, 10 mM $MgCl_2$, 10 mM DTT, 5% PEG, 10% DMSO), followed by the addition of 0.75 pmol target dsDNA (T1–T2), and adjusted to a final volume of 100 µl and incubated for 1 h at 37°C. After the incubation, the mixture was adjusted to a final volume of 200 µl with ELISA buffer (20 mM Tris [pH 8.0], 0.4 M NaCl, 10 mM EDTA, 0.1 mg/ml sonicated DNA). To harvest the strand-transfer product, the mixture was transferred into a 96-well micro titre plate coated with streptavidin (PIERCE, Rockford, IL, USA), followed by adding an alkaline phosphatase conjugated anti-DIG antibody (Roche Diagnostics, Mannheim, Germany) and a disodium 3-(4-methoxyspiro{1,2-dioxetane-3,2′-(5′-chloro)tricyclo[3.3.1.1^{3,7}]decan}-4-yl) phenyl phosphate (CSPD) substrate (Roche). The lumino-intensity was quantified with a Luminous CT-9000D luminometer (DIA-IATRON, Tokyo, Japan).

In addition to the above two different strand-transfer assays, a strand-transfer assay with radioisotope labelled target DNA and SDS-PAGE was employed in order to visually confirm the strand-transfer inhibition (Craigie *et al.*, 1995). By use of T4 polynucleotide kinase (TAKARA BIO, Osaka, Japan), the 5′ end of 20 mer target oligonucleotide-A (5′-TGTGGAAAATCTCTAGCAGT-3′) was labelled with [γ-^{32}P] ATP (370 MBq/µl, Amersham Bioscience, Tokyo, Japan). After the labelling reaction was terminated by adding EDTA, complementary oligonucleotide-B (5′-ACTGCTAGAGATTTTCCACA-3′) was added, and dsDNA was formed by heat denaturation and gradual cooling to room temperature. Unincorporated [γ-^{32}P]ATP was removed by G-25 Column (Amersham Bioscience, Piscataway, NJ). The reaction products were applied to 20% denatured polyacrylamide gel electrophoresis (300V/25A). The result of the electrophoresis was analysed by BAS-2500 (Fuji film, Tokyo, Japan).

Inhibition kinetics of IN

To analyse the strand-transfer inhibition mechanism of the test compounds, whether the action is competitive inhibition or non-competitive inhibition, Michaelis-Menten constant (K_m) and maximum velocity (V_{max}) were evaluated. Strand-transfer inhibition was evaluated on eight different time points (0, 1, 3, 5, 7.5, 10, 15, and 20 min) with four different compound concentrations (0, 1, 5, 10 µM) and target DNA concentrations (0.167, 0.25, 0.5, and 1 pmol). The initial reaction rate constants of IN were determined by linear regression using linear data points of product concentration–time plots. K_m and V_{max} were calculated from the Y-axis intercept in a plot of the slopes of Lineweaver-Burk analysis.

Intercalative activity evaluation

To clarify the possibility of intercalative activity of test compounds, ethidium bromide (EtBr) displacement assay was carried out following the protocol reported previously (Cain *et al.*, 1978). In brief, 1 µM calf thymus DNA (Invitrogen, Carlsbad, CA, USA) was mixed with EtBr (final concentration at 1.26 µM) and reaction buffer (2 mM HEPES, 10 µM EDTA, 9.4 mM NaCl, pH 7.0), and incubated for 10 min at room temperature. After the incubation, test compounds were added into the calf thymus DNA–EtBr mixture at different concentrations (final concentrations of 0.01–1000 µM). Fluorescence intensity of each mixture was determined by Fluoroskan Ascent FL (Helsinki, Finland. Excited at 544 nm, emitted at 590 nm). Actinomycin D (ICN Biomedical, Aurora, OH, USA), which is known as an intercalator, was employed as the positive control of the assay.

Molecular modelling studies

Molecular modelling studies were carried out using SYBYL software Version 6.9.1 (Tripos, St. Louis, MO, USA) running on an SGI Fuel workstation equipped with 600-MHz R14000 processor (SGI, Mountain View, CA, USA).

Evaluation of *in vitro* antiviral activity.

To evaluate HIV-1 replication inhibition by selected test compounds, *in vitro* antiviral assays were performed using a HeLa4.5/nEGFP reporter cell line. The HeLa4.5/nEGFP reporter cell line was established by transfection of CD4 and LTR driven EGFP reporter protein into the HeLa cell line. HeLa4.5/nEGFP reporter cells were maintained with D-MEM (Sigma) containing 5% FCS (Hyclone, Logan, UT, USA), 500 µg/ml G418, 1 µg/ml blasticidin and 2 µg/ml puromycin.

One day before conducting the assay, $1x10^4$ HeLa4.5/nEGFP cells were seeded into clear bottom black 96-well plates (NUNC, Rochester, NY, USA) with

200 μl/well medium and incubated at 37°C, 5% CO_2. The next day, 1250 $TCID_{50}$ HXB2 were added in each well, followed by addition of the test compounds in final concentrations of 5, 1, 0.2, 0.04, 0.008, 0.0016, 0.00032, and 0.000064 μM. Forty-eight hours after infection, the cells were fixed by 3.2% formaldehyde and the nuclei of cells were stained by 10 μg/ml Hoechst33342 (Molecular Probes, Engene, OR, USA). EGFP positive cell number ($EGFP^+$) and Hoechst33342 positive cell number ($hoechst33342^+$) were determined by Cellomics Array Scan, HSC Systems (Beckman Coulter, Tokyo, Japan).

Inhibitory activity of each compound was determined by the following formula:

% inhibition = 1 − {($EGFP^+$ cell number with drug/$hoechst33342^+$ cell number with drug) − ($EGFP^+$ cell number without infection/$hoechst33342^+$ cell number without infection)}/{($EGFP^+$ cell number without drug/$hoechst33342^+$ cell number without drug) − ($EGFP^+$ cell number without infection/$hoechst33342^+$ cell number without infection)}.

Results

A small molecule bearing a carbazole moiety demonstrated strand-transfer inhibitory activity

A diverse library of 12 000 small-molecule compounds was screened for strand-transfer inhibitory activity at 100 μM concentration by M8 apparatus. Seventy-two compounds that demonstrated more than 80% strand-transfer-inhibition were selected and applied to the second screening using in-house strand-transfer assay. In the second screening, to confirm dose-dependent inhibition of the test compounds, each compound was tested at four different concentrations. Of the 72 compounds, a compound bearing a carbazole moiety, 8-chloro-2-[2-(dimethylamino)ethyl]-9-hydroxy-5-methylpyrrolo[3,4-c]carbazole-1,3(2H,6H)-dione (coded as **CA-0**), was found to demonstrate potent strand-transfer inhibitory activity (Figure 1A). As shown in Figure 1B, **CA-0** demonstrated clear dose-dependent inhibition of the strand-transfer reaction with an IC_{50} of 5.00 ±3.31 μM. The dose-dependent inhibition was also confirmed by SDS-PAGE with [γ-^{32}P] labelled target DNA. As demonstrated in Figure 1C, strand-transferred product bands diminished along with increased concentration of the inhibitor. IC_{50} value determined from intensities of the bands was 1.24 ±0.09 μM, which was consistent with that evaluated via the plate assay.

Strand-transfer inhibition of 23 carbazole derivatives, and the relationship between their structures and inhibitory activity

To understand the relationship between structure and strand-transfer inhibition activity, we selected 23 carbazole

Figure 1. Structure and strand transfer inhibitory activity of 8-chloro-2-[2-(dimethylamino) ethyl]-9-hydroxy-5-methylpyrrolo[3,4-c]carbazole-1,3(2H,6H)-dione (**CA-0**)

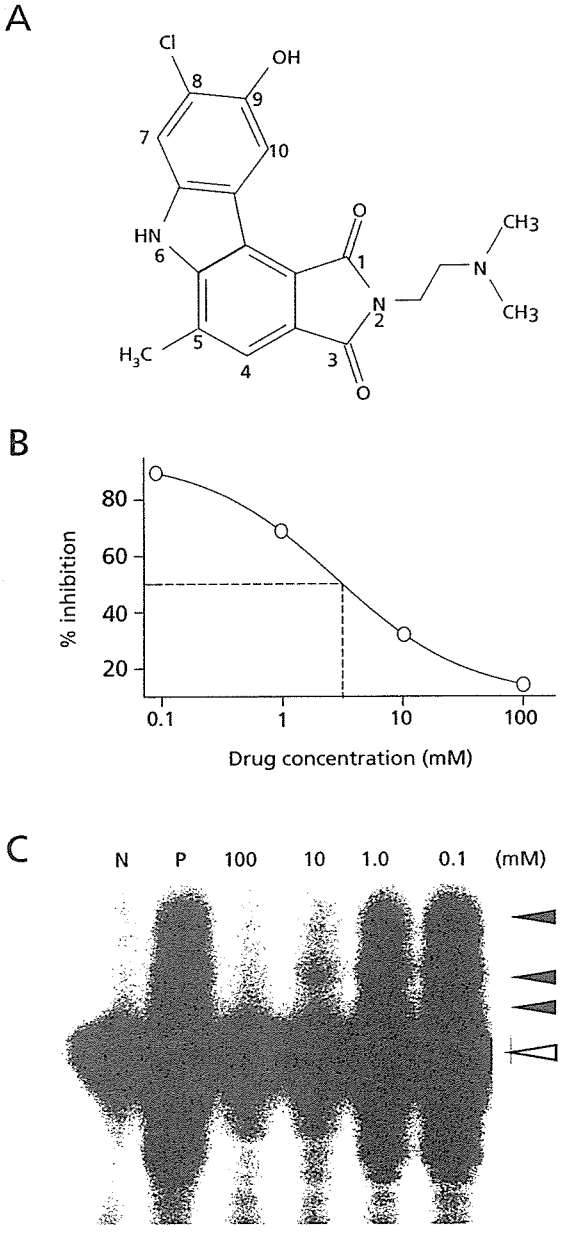

(A) The structure of **CA-0**, a strand transfer inhibitory compound identified from among a library of 12 000 small molecular weight compounds. It has a carbazole structure as a scaffold. The small numbers written beside the structure indicate the residue number of the compound. **(B)** A dose–response curve of **CA-0**. The dotted line indicates the IC_{50} point of the chemical, which was 5.00 ±3.31 μM. **(C)** A strand transfer assay by radioisotope-labelled oligonuceotide. Lane 1 "N" stands for the negative control, with only a radioisotope-labelled nucleotide. Lane 2 "P" stands for positive control, with radioisotope-labelled nucleotide and recombinant integrase. Lanes 3 to 6 were with inhibitor. The open triangle and solid triangle indicate labelled oligonucelotide and strand transfer products, respectively.

derivatives with different substituents. As demonstrated in Figure 2, all compounds had pyrrolo[3,4-c]carbazole structures as scaffolds, and all except **CA-5**, **CA-10** and **CA-19** had 2-dimethylaminoethyl group at position R2. Six of the 23 compounds demonstrated potent strand-transfer inhibition comparable to that of **CA-0**. These compounds were **CA-1**, **CA-4**, **CA-8**, **CA-9**, **CA-12** and **CA-13**. IC_{50} values of these test compounds were similar with positive control S-1360. Moderate inhibitory activities were observed in twelve compounds, **CA-2**, **CA-3**, **CA-7**, **CA-11**, **CA-14**, **CA-15**, **CA-16**, **CA-17**, **CA-18**, **CA-21**, **CA-22** and **CA-23**. Five compounds, **CA-5**, **CA-6**, **CA-10**, **CA-19** and **CA-20**, did not show significant inhibition, even at the highest concentration tested

Figure 2. Structures of **CA-0** and 23 carbazole derivatives evaluated for strand transfer inhibitory activity

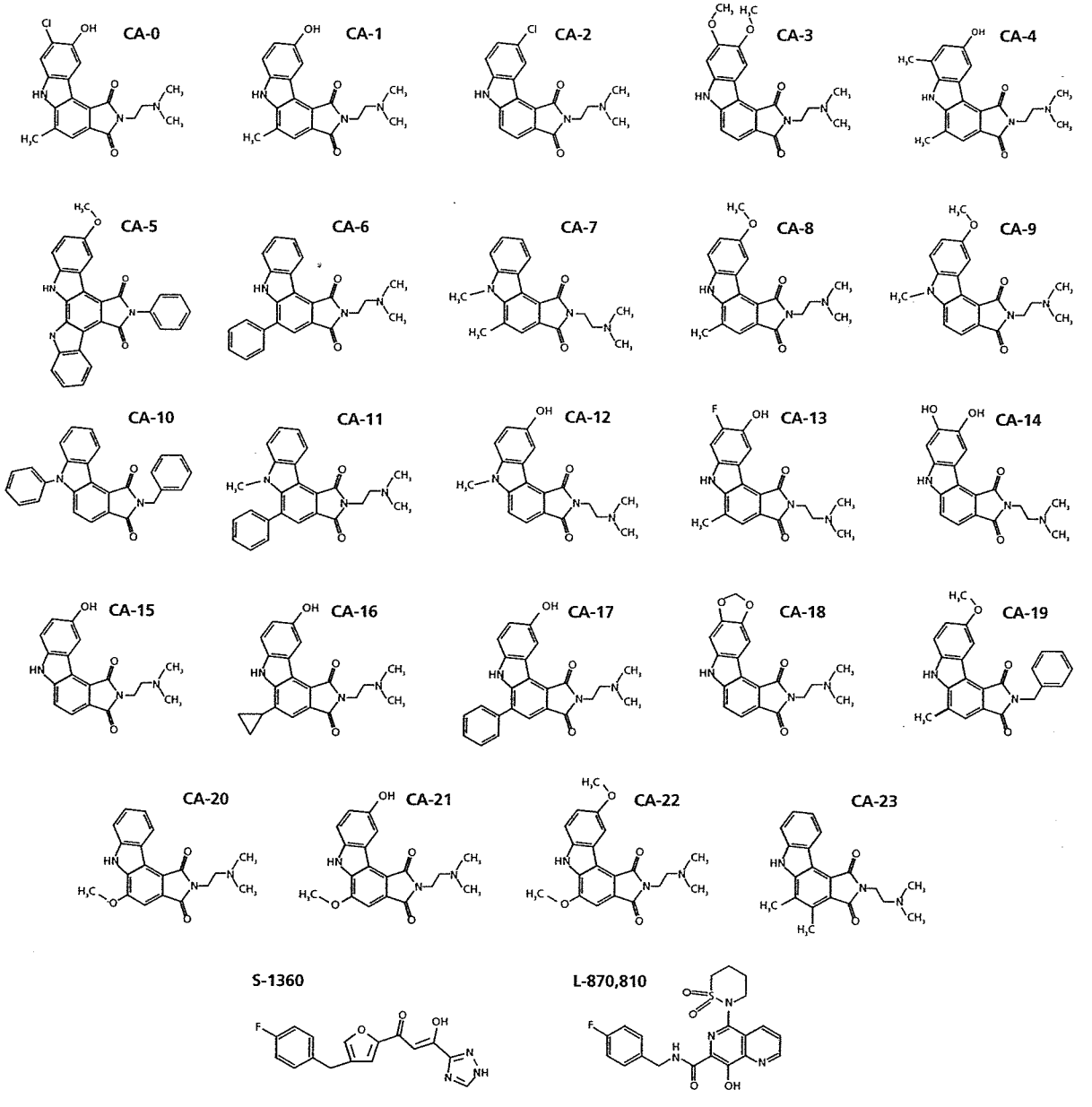

CA-0 and 23 related compounds with carbazole scaffold tested for strand-transfer inhibitory activities are depicted. S-1360 and L-870,810, which have previously been reported as potent IN inhibitors, are also shown.

(100 μM). The compounds that demonstrated potent strand-transfer inhibitory activity were also confirmed by gel-based assay, and IC_{50} values determined from the gel-based assay were consistent with the values determined via in-house plate assay (Table 1).

Carbazole derivatives are competitive inhibitors of integrase

To investigate the strand-transfer inhibitory mechanisms and kinetics of the compounds, we determined V_{max} and K_m of the inhibition by Lineweaver–Burke plot analyses. We selected two compounds, **CA-0** and **CA-13**, for the analyses. As summarized in Table 2, larger K_m values (nM) were observed with higher inhibitory concentration, whereas V_{max} values (RU/min) did not change and remained consistent at any inhibitory concentration (Figure 3). As shown in Figure 3A and 3B, data-fitted lines of different time points converged on the Y axis, indicating that **CA-0** and **CA-13** inhibited strand-transfer in a competitive manner.

Table 1. Strand transfer and *in vitro* viral replication inhibitory activities of carbazole derivatives

	IC_{50} in strand transfer assay		Anti-HIV activity
	Plate assay (μM)	Gel assay (μM)	IC_{50} (μM)
(A) High-inhibitory group			
CA-0	5.00 ±3.31	1.24 ±0.09	0.48 ±0.06
CA-13	4.38 ±2.78	1.13 ±0.21	0.51 ±0.12
CA-1	7.94 ±4.12	2.97 ±0.21	0.92 ±0.15
CA-4	8.99 ±3.39	6.34 ±0.89	1.52 ±0.46
CA-8	6.61 ±4.17	6.38 ±0.32	0.79 ±0.07
CA-9	4.42 ±1.87	4.10 ±0.46	0.80 ±0.11
CA-12	5.93 ±3.53	3.14 ±0.04	0.69 ±0.15
(B) Intermediate-inhibitory group			
CA-2	22.50 ±2.27	ND	ND
CA-3	72.69 ±5.44	ND	ND
CA-7	11.88 ±7.66	ND	ND
CA-11	57.00 ±3.13	ND	ND
CA-14	17.37 ±1.79	ND	ND
CA-15	27.28 ±9.10	ND	ND
CA-16	20.51 ±15.11	ND	ND
CA-17	50.64 ±19.02	ND	ND
CA-18	10.68 ±8.88	ND	ND
CA-21	25.01 ±10.60	ND	ND
CA-22	16.92 ±7.32	ND	ND
CA-23	16.94 ±7.82	ND	ND
(C) Intermediate-inhibitory group			
CA-5	>100	ND	ND
CA-6	>100	ND	ND
CA-10	>100	ND	ND
CA-19	>100	ND	ND
CA-20	>100	ND	ND
(D) Previously reported inhibitor			
S-1360	4.67 ±1.89	ND	ND

Underline, indicates original compound; IC_{50}, 50% inhibition concentration; ND, not done.

Carbazole derivates have not shown intercalative activity

Due to their planar structure and their manner of competitive inhibition, we were concerned that the compounds might have the intercalative activity to destroy substrate dsDNA, rather than binding to the IN to block its enzyme activity. To clear the possibility of the intercalation, EtBr displacement assay was carried out. Since EtBr intercalates into dsDNA and makes visualization possible by growing fluorescence under UV light, intercalative activity of the test compounds can be evaluated by whether the test compounds displace incorporated EtBr out from dsDNA. As shown in Figure 4, fluorescence intensity diminished in a dose-dependent manner by actinomycin D, a compound known as a potent intercalator. In contrast, our two test compounds **CA-0** and **CA-13** did not affect fluorescence intensity, even at the highest concentration of 1 mM, suggesting that **CA-0** and **CA-13** were not intercalators.

Antiviral activity

We employed a single replication infectivity assay using HeLa4.5/EGFP cells to investigate the potency of antiviral activity. IC_{50} values of **CA-0** and the six compounds were 0.48, 0.92, 1.52, 0.79, 0.8, 0.69, 0.51 μM, respectively. The IC_{50} values of all seven compounds were 5.5 to 10.4-fold lower than that of the strand transfer assay (Table 1A). The discrepancy in IC_{50} between the two assays can be explained by stoichiometry of the inhibitor and the target enzyme in the two assays, and the estimated amount of IN in-strand transfer assay was higher than in the

Table 2. Inhibition kinetics of representative carbazole compounds **CA-0** and **CA-13**

Chemical	Concentration	V_{max} (RU/min)	K_m (nM)
CA-0	10 μM	463.16 ±63.16	30.40 ±7.80
	5 μM	402.58 ±32.21	26.21 ±7.40
	1 μM	370.14 ±84.42	12.71 ±2.02
	0 μM	454.55 ±0.02	9.18 ±1.18
CA-13	10 μM	409.70 ±35.47	19.31 ±4.68
	5 μM	439.07 ±164.74	14.83 ±0.24
	1 μM	438.08 ±53.85	11.09 ±2.42
	0 μM	429.83 ±136.46	7.08 ±0.64

Figure 3. Inhibition kinetics assays of two representative carbazole derivatives, **CA-0** and **CA-13**

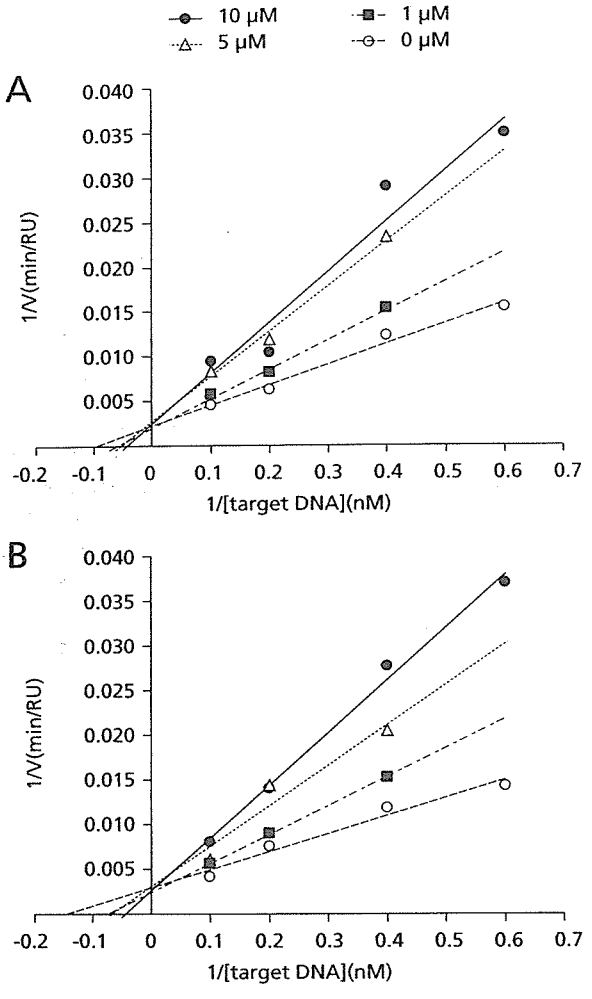

Lineweaver–Burke plot analyses of **(A) CA-0** and **(B) CA-13** are depicted.

Figure 4. Ethidium bromide displacement assays of two representative carbazole derivatives, **CA-0** and **CA-13**

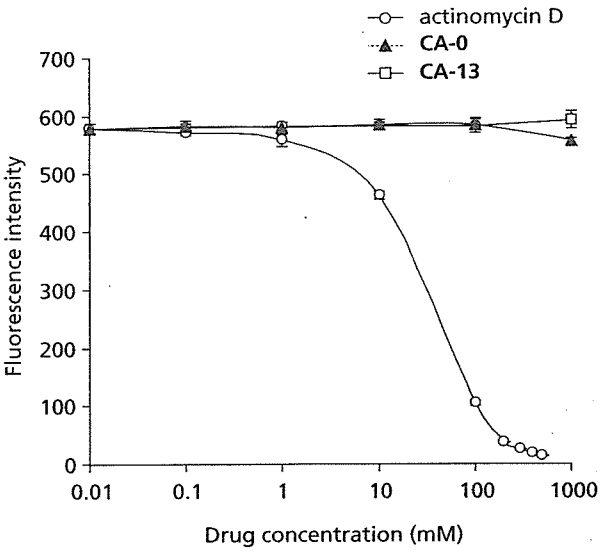

To evaluate intercalative activities of carbazole derivatives, ethidium bromide displacement assays were carried out for two representative compounds, **CA-0** and **CA-13**.

HeLa4.5/EGFP assay. Seven compounds exhibited considerable toxicity, suggesting that efforts toward decreasing toxicity are necessary for the further development of carbazole-based inhibitors.

Discussion

Carbazole, a fused phenyl-ring structure with hydrophobicity, has provided an interesting scaffold for the development of novel drugs. Staurosporine, discovered among microbial alkaloids, was the first carbazole derivative reported to demonstrate biological activity (Omura *et al.*, 1977; Furusaki *et al.*, 1978; Furusaki *et al.*, 1982), which was protein kinase C inhibition (Tamaoki *et al.*, 1986). Other carbazole derivatives have demonstrated various other activities, such as topoisomerase inhibition (Marotto *et al.*, 2002; Facompre *et al.*, 2002; Carrasco *et al.*, 2001), hypotensive activity (Furusaki *et al.*, 1982), platelet aggregation inhibition (Oka *et al.*, 1986), and anti-fungal activity (Sunthitikawinsakul *et al.*, 2003). In this report we present another possible activity of carbazole derivatives, that of HIV-1 integrase inhibitor.

As compounds with three or four fused aromatic ring structures have been reported to demonstrate intercalative activity (Fukui & Tanaka, 1996; Dziegielewski *et al.*, 2002), we initially suspected that our carbazole derivatives also have intercalative activities, penetrating and disturbing target dsDNA, resulting in pseudo strand-transfer inhibition. Indeed, several carbazole derivatives have been recognized to demonstrate intercalative activity (Facompre *et al.*, 2002; Long *et al.*, 2002). We confirmed that actinomycin D, which is a well-known intercalator (Ross *et al.*, 1979; Wilson & Jones, 1982), demonstrated strand-transfer inhibition in our assay (data not shown). However, taking into consideration the data that our carbazole derivatives inhibited strand-transfer in a competitive manner, and also that the compounds could not displace EtBr out from dsDNA, we assume that our derivatives bind to part of the IN molecule, to the region responsible for DNA target

binding or to the catalytic site responsible for strand-transfer activity.

To understand in greater detail the substituents responsible for strand-transfer inhibitory activity, we analysed 23 carbazole derivatives, and classified them into three categories according to their levels of inhibition (Table 1). Six compounds were classified as the high-inhibition group, which demonstrated IC_{50} of less than 10 μM, 12 compounds were classified as the intermediate group, which demonstrated IC_{50} of greater than 10 μM and less than 100 μM, and five compounds were classified as the non-inhibition group, in which we did not observe significant inhibition even at the highest concentration tested (100 μM).

Comparing the compounds between and within these three categories, we recognized three factors responsible for strand-transfer inhibition. The first and most important factor is the incidence of a 2-dimethylaminoethyl group at position R2 (Figure 1A).

CA-8, which possesses a 2-dimethylaminoethyl group at position R2, demonstrated high inhibitory activity (IC_{50}: 6.61 ±4.17 μM), but **CA-19** (IC_{50}: >100 μM), which possesses a phenyl ring structure at the same R2 position, did not demonstrate inhibitory activity. Thus, it is clear that the incidence of a 2-dimethylaminoethyl group, which has a basic property, is critical for strand-transfer inhibition activity. Indeed, we recognized that all compounds in the "high-inhibitory group" and "intermediate-inhibitory group" had this basic substituent at position R2 (Table 1A, 1B, Figure 2). In contrast, three of five compounds in the "non-inhibitory group" had the phenyl ring structure at R2 position. It is thought that these compounds might bind to the acidic region on the IN molecule and compete with the target dsDNA.

The second factor is the incidence of a methyl (Me) group at position R5, R6 or R7. We recognized that compounds in the high inhibitory group had at least one Me group at the R5, R6 or R7 position (Table 1A, Figure 2). Comparing **CA-1** (IC_{50}: 7.94 ±4.12 μM), **CA-4** (IC_{50}: 8.99 ±3.39 μM), and **CA-12** (IC_{50}: 5.93 ±3.53 μM) with **CA-15** (IC_{50}: 27.28 ±9.10 μM), it is clear that the incidence of an Me group within the R5 to R7 positions was an important factor for enhanced inhibitory activity. It seems that the position of the substituent may not be critical between R5 and R6, as we did not see significant differences between **CA-1** (IC_{50}: 7.94 ±4.12 μM) and **CA-12** (IC_{50}: 5.93 ±3.53 μM), and also between **CA-8** (IC_{50}: 6.61 ±4.17 μM) and **CA-9** (IC_{50}: 4.42 ±1.87 μM).

According to the IC_{50} levels of **CA-5** (>100 μM), **CA-6** (>100 μM) and **CA-11** (>100 μM), it appears that bulky substituents at the R5 position have a negative effect on inhibition (Table 1C, Figure 2). Furthermore, the inhibition potential of the three compounds **CA-1** (IC_{50}: 7.94 ±4.12 μM), **CA-16** (IC_{50}: 20.51 ±15.11 μM) and **CA-17** (IC_{50}: 50.64 ±19.02 μM) depended on the molecular size of their R5 substituents. It is probable that the R5 substituents of these compounds were too large and that they interfered with surrounding molecules forming the binding site (Table 1A, 1B, Figure 2). These data indicate that the binding site of carbazole might have a space limitation, and thus the size and shape of the molecules may be important factors for inhibitor activity.

The third factor is the substituent at position R9. Comparing **CA-20** (IC_{50}: >100 μM), **CA-21** (IC_{50}: 25.01 ±10.60 μM) and **CA-22** (IC_{50}: 16.92 ±7.32 μM), these three compounds were identical, with the exception of the substituent at position R9 (Table 1B, 1C, Figure 2). **CA-21** and **CA-22** have hydroxyl residue and a methoxy group at position R9, respectively. We noticed a significant difference in inhibitory activity between **CA-20** and **CA-21**, and between **CA-20** and **CA-22**, suggesting the possibility that both the hydroxyl group and the methoxy group at R9 formed hydrogen bonds with the amino acid molecules forming the binding sites, as these two substituents have the potential to be hydrogen bond acceptors. It appears that hydroxyl and methoxy groups have similar effects on strand-transfer inhibitory activities. In addition to the above three factors, we found that molecular interaction between R8 and R9 substituents, and their arrangement, are also important determinants for efficient inhibitory activity. **CA-3**, with two methoxy groups at R8 and R9, appears to have a bulky arrangement of the two side chains, and demonstrated an IC_{50} of 72.69 ±5.44 μM, whereas **CA-14** and **CA-18**, which were expected to have horizontal arrangements, demonstrated lower IC_{50} values of 17.37 ±1.79 μM and 10.68 ±8.88 μM, respectively (Table 1B, Figure 2).

To summarize these structural elements, and to understand the common structure of molecules that demonstrated strand-transfer inhibitory activity, we superposed inhibitor structures having significant strand-transfer inhibition (**CA-0**, **CA-1**, **CA-4**, **CA-8**, **CA-9**, **CA-12** and **CA-13**) (Figure 5A), and the structures of compounds with no inhibition (**CA-5**, **CA-6**, **CA-10**, **CA-19** and **CA-20**) (Figure 5B). In comparing these two overlapped figures, we found that the compounds with inhibitory activity share a largely identical structure and similar molecular size. In contrast, the non-inhibitory compounds had larger and more uneven-shaped side chains. Overall, the superposed structures indicate that the molecules should be planar and have basic diethylaminoethyl groups to demonstrate strand-transfer inhibitory activity.

In conclusion, we have identified a small molecular weight compound with a carbazole scaffold, which can be the lead compound for developing novel IN inhibitors. Furthermore, analysing the IN inhibitory mechanisms of

Figure 5. A structural comparison between high/intermediate inhibitory compounds and non-inhibitory compounds

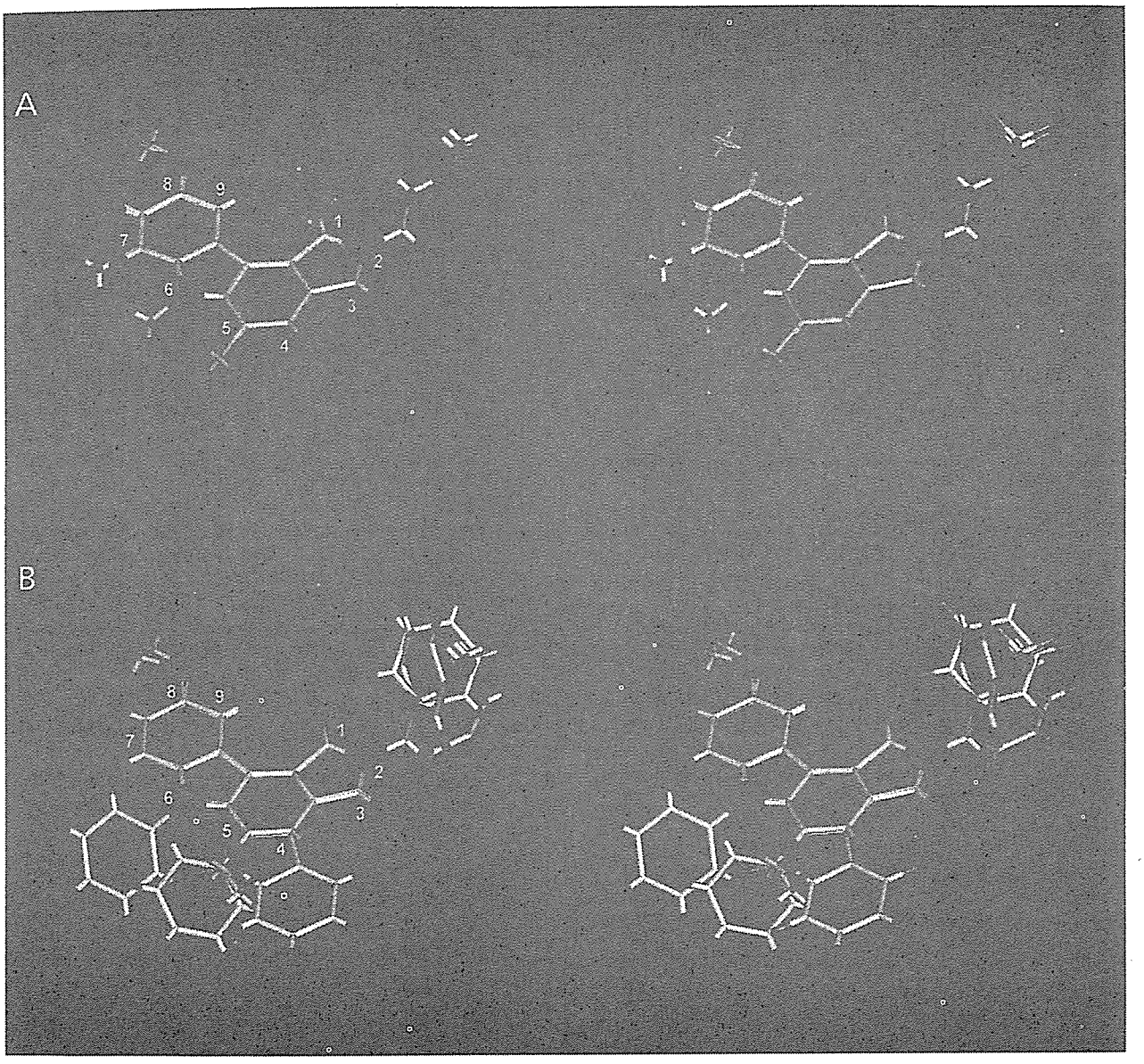

Superposed structures of **(A)** five non-inhibitory compounds, **CA-5, 6, 10, 19** and **20**, and **(B)** seven inhibitory compounds, **CA-0, 1, 4, 8, 9, 12** and **13**, are demonstrated in stereo-view images. In both figures, residue numbers are indicated beside the structures. Red, dark blue and light blue indicate oxygen, nitrogen and hydrogen molecules, respectively. Green indicates chlorine or fluorine molecules. SYBYL software Version 6.9.1 running on an SGI Fuel workstation was used to construct the figures.

carbazole derivatives may yield more detailed information regarding HIV-1 IN structure and function.

Acknowledgements

This study was supported by a grant from the Human Sciences Foundation, the Organization of Pharmaceutical Safety and Research of Japan and the Ministry of Health, Labor and Welfare of Japanese Government. This study was partly supported by the Program for Promotion of Fundamental Studies in Health Sciences of the National Institute of Biomedical Innovation (NIBIO)

We would like to thank Dr. Haruo Tanaka and Takuro Shiomi, professor and associate professor of Kitazato

Institute, for their valuable advice and comments. We would also like to thank the laboratory members of Toyama Chemical Co. Ltd. for supplying the compounds in the study. Finally, we would like to thank Ms. Mary Phillips and Ms. Yumi Fujiuji for preparing the manuscript.

References

Balzarini J (2004) Current status of the non-nucleoside reverse transcriptase inhibitors of human immunodeficiency virus type 1. *Current Topics in Medicinal Chemistry* **4**:921–944.

Burke CJ, Sanyal G, Bruner MW, Ryan JA, LaFemina RL, Robbins HL, Zeft AS, Middaugh CR & Cordingley MG (1992) Structural implications of spectroscopic characterization of a putative zinc finger peptide from HIV-1 integrase. *The Journal of Biological Chemistry* **267**:9639–9644.

Cain BF, Baguley BC & Denny WA (1978) Potential antitumor agent. 28. deoxyribonucleic acid polyintercalating agents. *Journal of Medicinal Chemistry* **21**:658–668.

Carrasco C, Vezin H, Wilson WD, Ren J, Chaires JB & Bailly C (2001) DNA binding properties of the indolocarbazole antitumor drug NB-506. *Anticancer Drug Design* **16**:99–107.

Chun TW, Finzi D, Margolick J, Chadwick K, Schwartz D & Siliciano RF (1995) *In vivo* fate of HIV-1-infected T cells: quantitative analysis of the transition to stable latency. *Nature Medicine* **1**:1284–1290.

Craigie R, Hickman AB & Engelman A (1995) Integrase. in *HIV: A Practical Approach – Volume 2: Biochemistry, Molecular Biology, and Drug Discovery*; pp. 53–71. Edited by J Karn. New York: Oxford University Press.

Dayam R & Neamati N (2003) Small-molecule HIV-1 integrase inhibitors: the 2001–2002 update. *Current Pharmacology Design* **9**:1789–1802.

De Clercq E (1992) HIV inhibitors targeted at the reverse transcriptase. *AIDS Research and Human Retroviruses* **8**:119–134.

Dziegielewski J, Slusarski B, Konitz A, Skladanowski A & Konopa J (2002) Intercalation of imidazoacridinones to DNA and its relevance to cytotoxic and antitumor activity. *Biochemical Pharmacology* **63**:1653–1662.

Engelman A & Craigie R (1992) Identification of conserved amino acid residues critical for human immunodeficiency virus type 1 integrase function *in vitro*. *Journal of Virology* **66**:6361–6369.

Engelman A, Englund G, Orenstein JM, Martin MA & Craigie R (1995) Multiple effects of mutations in human immunodeficiency virus type 1 integrase on viral replication. *Journal of Virology* **69**:2729–2736.

Engelman A, Hickman AB & Craigie R (1994) The core and carboxyl-terminal domains of the integrase protein of human immunodeficiency virus type 1 each contribute to nonspecific DNA binding. *Journal of Virology* **68**:5911–5917.

Facompre M, Carrasco C, Colson P, Houssier C, Chisholm JD, Van Vranken DL & Bailly C (2002) DNA binding and topoisomerase I poisoning activities of novel disaccharide indolocarbazoles. *Molecular Pharmacology* **62**:1215–1227.

Fukui K & Tanaka K (1996) The acridine ring selectively intercalated into a DNA helix at various types of abasic sites: double strand formation and photophysical properties. *Nucleic Acids Research* **24**:3962–3967.

Furusaki A, Hashiba N, Matsumoto T, Hirano A, Iwai Y & Omura S (1978) X-ray crystal structure of staurosporine: a new alkaloid from a Streptomyces strains. *Journal of the Chemical Society. Chemical Communications* 800–801.

Furusaki A, Hashiba N, Matsumoto T, Hirano A, Iwai Y & Omura S (1982) The crystal and molecular structure of staurosporine, a new alkaloid from a Streptomyces strains. *Bulletin of the Chemical Society of Japan* **55**:3681–3685.

Goldgur Y, Craigie R, Cohen GH, Fujiwara T, Yoshinaga T, Fujishita T, Sugimoto H, Endo T, Murai H & Davies DR (1999) Structure of the HIV-1 integrase catalytic domain complexed with an inhibitor: a platform for antiviral drug design. *Proceedings of the National Academy of Sciences, USA* **96**:13040–13043.

Grobler JA, Stillmock K, Hu B, Witmer M, Felock P, Espeseth AS, Wolfe A, Egbertson M, Bourgeois M, Melamed J, Wai JS, Young S, Vacca J & Hazuda DJ (2002) Diketo acid inhibitor mechanism and HIV-1 integrase: implications for metal binding in the active site of phosphotransferase enzymes. *Proceedings of the National Academy of Sciences USA* **99**:6661–6666.

Hazuda DJ, Anthony NJ, Gomez RP, Jolly SM, Wai JS, Zhuang L, Fisher TE, Embrey M, Guare JP, Jr., Egbertson MS, Vacca JP, Huff JR, Felock PJ, Witmer MV, Stillmock KA, Danovich R, Grobler J, Miller MD, Espeseth AS, Jin L, Chen IW, Lin JH, Kassahun K, Ellis JD, Wong BK, Xu W, Pearson PG, Schleif WA, Cortese R, Emini E, Summa V, Holloway MK & Young SD (2004) A naphthyridine carboxamide provides evidence for discordant resistance between mechanistically identical inhibitors of HIV-1 integrase. *Proceedings of the National Academy of Sciences USA* **101**:11233–11238.

Hazuda DJ, Felock P, Witmer M, Wolfe A, Stillmock K, Grobler JA, Espeseth A, Gabryelski L, Schleif W, Blau C & Miller MD (2000) Inhibitors of strand transfer that prevent integration and inhibit HIV-1 replication in cells. *Science* **287**:646–650.

Imamichi T (2004) Action of anti-HIV drugs and resistance: reverse transcriptase inhibitors and protease inhibitors. *Current Pharmaceutical Design* **10**:4039–4053.

Johnson AA, Marchand C & Pommier Y (2004) HIV-1 integrase inhibitors: a decade of research and two drugs in clinical trial. *Current Topics in Medicinal Chemistry* **4**:1059–1077.

Khan E, Mack JP, Katz RA, Kulkosky J & Skalka AM (1991) Retroviral integrase domains: DNA binding and the recognition of LTR sequences. *Nucleic Acids Research* **19**:851–860.

Kohl NE, Emini EA, Schleif WA, Davis LJ, Heimbach JC, Dixon RA, Scolnick EM & Sigal IS (1988) Active human immunodeficiency virus protease is required for viral infectivity. *Proceedings of National Academy of Sciences USA* **85**:4686–4690.

LaFemina RL, Schneider CL, Robbins HL, Callahan PL, LeGrow K, Roth E, Schleif WA & Emini EA (1992) Requirement of active human immunodeficiency virus type 1 integrase enzyme for productive infection of human T-lymphoid cells. *Journal of Virology* **66**:7414–7419.

Long BH, Rose WC, Vyas DM, Matson JA & Forenza S (2002) Discovery of antitumor indolocarbazoles: rebeccamycin, NSC 655649, and fluoroindolocarbazoles. *Current Medicinal Chemistry. Anti-Cancer Agents* **2**:255–266.

Marotto A, Kim YS, Schulze E & Pindur U (2002) New indolocarbazoles as antitumour active compounds: evaluation of the target by experimental and theoretical studies. *Pharmazie* **57**:194–197.

Oka S, Kodama M, Takeda H, Tomizuka N & Suzuki H (1986) Staurosporine, a potent platelet aggregation inhibitor form a *Streptomyces* species. *Agricultural and Biological Chemistry* **50**:2723–2727.

Omura S, Iwai Y, Hirano A, Nakagawa A, Awaya J, Tsuchya H, Takahashi Y & Masuma R (1977) A new alkaloid AM-2282 of *Streptomyces* origin. Taxonomy, fermentation, isolation and preliminary characterization. *The Journal of Antibiotics (Tokyo)* **30**:275–282.

Pluymers W, Pais G, Van Maele B, Pannecouque C, Fikkert V, Burke TR, Jr., De Clercq E, Witvrouw M, Neamati N & Debyser Z (2002) Inhibition of human immunodeficiency virus type 1 integration by diketo derivatives. *Antimicrobial Agents and Chemotherapy* **46**:3292–3297.

Pommier Y, Marchand C & Neamati N (2000) Retroviral integrase inhibitors year 2000: update and perspectives. *Antiviral Research* **47**:139–148.

Ross WE, Glaubiger D & Kohn KW (1979) Qualitative and quantitative aspects of intercalator-induced DNA strand breaks. *Biochimica et Biophyssica Acta* **562**:41–50.

Ruscetti FW (1985) Immunopathology associated with human lymphotropic retroviruses. *Survey and Synthesis of Pathology Research* **4**:216–226.

Schauer M & Billich A (1992) The N-terminal region of HIV-1 integrase is required for integration activity, but not for DNA-binding. *Biochemical and Biophysical Research Communications* **185**:874–880.

Sunthitikawinsakul A, Kongkathip N, Kongkathip B, Phonnakhu S, Daly JW, Spande TF, Nimit Y & Rochanaruangrai S (2003) Coumarins and carbazoles from *Clausena excavata* exhibited antimycobacterial and antifungal activities. *Planta Medica* **69**:155–157.

Tamaoki T, Nomoto H, Takahashi I, Kato Y, Morimoto M & Tomita F (1986) Staurosporine, a potent inhibitor of phospholipid/Ca^{++} dependent protein kinase. *Biochemical and Biophysical Research Communications* **135**:397–402.

Tronchet JM & Seman M (2003) Non-nucleoside inhibitors of HIV-1 reverse transcriptase: from the biology of reverse transcription to molecular design. *Current Topics in Medicinal Chemistry* **3**:1496–1511.

Wilson WD & Jones RL (1982) Interaction of actinomycin D, ethidium, quinacrine, daunorubicin, and tetralysine with DNA: 31P NMR chemical shift and relaxation investigation. *Nucleic Acids Research* **10**:1399–1410.

Woerner AM & Marcus-Sekura CJ (1993) Characterization of a DNA binding domain in the C-terminus of HIV-1 integrase by deletion mutagenesis. *Nucleic Acids Research* **21**:3507–3511.

Received 22 August 2005, accepted 27 September 2005

JOURNAL OF VIROLOGY, Feb. 2005, p. 1452–1462
0022-538X/05/$08.00+0 doi:10.1128/JVI.79.3.1452–1462.2005

Vol. 79, No. 3

Vaccination of Rhesus Macaques with Recombinant *Mycobacterium bovis* Bacillus Calmette-Guérin Env V3 Elicits Neutralizing Antibody-Mediated Protection against Simian-Human Immunodeficiency Virus with a Homologous but Not a Heterologous V3 Motif

Kenji Someya,[1]* Dayaraj Cecilia,[2] Yasushi Ami,[3] Tadashi Nakasone,[1] Kazuhiro Matsuo,[1,4] Sherri Burda,[2] Hiroshi Yamamoto,[5] Naoto Yoshino,[6] Masahiko Kaizu,[1,4] Shuji Ando,[1] Kenji Okuda,[7] Susan Zolla-Pazner,[2] Shudo Yamazaki,[1] Naoki Yamamoto,[1] and Mitsuo Honda[1,4]

AIDS Research Center[1] and Division of Experimental Animal Research,[3] National Institute of Infectious Diseases, Shinjuku-ku, Tokyo, Yokohama City University, Kanazawa-ku, Yokohama,[7] Japan Science and Technology Corporation, Kawaguchi, Saitama,[4] Toyama Medical Pharmaceutical University, Toyama, Toyama,[5] and Iwate Medical University, Morioka, Iwate,[6] Japan, and New York University Medical Center, New York, New York[2]

Received 25 June 2004/Accepted 23 September 2004

Although the correlates of vaccine-induced protection against human immunodeficiency virus type 1 (HIV-1) are not fully known, it is presumed that neutralizing antibodies (NAb) play a role in controlling virus infection. In this study, we examined immune responses elicited in rhesus macaques following vaccination with recombinant *Mycobacterium bovis* bacillus Calmette-Guérin expressing an HIV-1 Env V3 antigen (rBCG Env V3). We also determined the effect of vaccination on protection against challenge with either a simian-human immunodeficiency virus (SHIV-MN) or a highly pathogenic SHIV strain (SHIV-89.6PD). Immunization with rBCG Env V3 elicited significant levels of NAb for the 24 weeks tested that were predominantly HIV-1 type specific. Sera from the immunized macaques neutralized primary HIV-1 isolates in vitro, including HIV-$1_{BZ167/X4}$, HIV-$1_{SF2/X4}$, HIV-$1_{CI2/X4}$, and, to a lesser extent, HIV-$1_{MNp/X4}$, all of which contain a V3 sequence homologous to that of rBCG Env V3. In contrast, neutralization was not observed against HIV-$1_{SF33/X4}$, which has a heterologous V3 sequence, nor was it found against primary HIV-1 R5 isolates from either clade A or B. Furthermore, the viral load in the vaccinated macaques was significantly reduced following low-dose challenge with SHIV-MN, and early plasma viremia was markedly decreased after high-dose SHIV-MN challenge. In contrast, replication of pathogenic SHIV-89.6PD was not affected by vaccination in any of the macaques. Thus, we have shown that immunization with an rBCG Env V3 vaccine elicits a strong, type-specific V3 NAb response in rhesus macaques. While this response was not sufficient to provide protection against a pathogenic SHIV challenge, it was able to significantly reduce the viral load in macaques following challenge with a nonpathogenic SHIV. These observations suggest that rBCG vectors have the potential to deliver an appropriate virus immunogen for desirable immune elicitations.

Development of a preventive vaccine against human immunodeficiency virus type 1 (HIV-1) is urgently needed to control the spread of the virus worldwide. Although the immunological parameters that correlate with protective immunity against natural infection with HIV-1 are not fully known, it is assumed that a preventive vaccine must elicit potent, broadly reactive immunity against divergent strains of HIV-1 (25, 36, 42). Several recent studies have demonstrated that induction of virus-specific T-cell responses can confer protective immunity in nonhuman primate models, and these responses may also play a role in controlling HIV-1 replication in humans (6, 18, 19, 31, 33, 34, 38, 45, 48). Vaccine constructs containing viral *env* genes, in addition to *gag* and *pol*, have been shown to effectively control replication of challenge viruses (2, 5, 10), suggesting that neutralizing antibody (NAb) responses might also contribute to protection against pathogenic infection or disease progression. Passive transfer of serum immunoglobulin from chimpanzees experimentally infected with several different HIV-1 isolates has been shown to block the establishment of a simian immunodeficiency virus (SIV)-HIV chimeric simian-human immunodeficiency virus (SHIV) infection in pig-tailed macaques (37, 46). It is not known, however, whether vaccines that actively elicit a potent NAb response can provide protection in nonhuman primates challenged with SHIV.

Previously, we demonstrated that recombinant *Mycobacterium bovis* bacillus Calmette-Guérin (rBCG), which secretes a chimeric protein consisting of the V3-neutralizing epitope of HIV-1 and α-antigen (rBCG Env V3), can induce HIV-1-specific NAb in a small-animal model (9, 15, 16). BCG was selected as a vaccine vehicle because it has several characteristics that are considered efficacious for developing a candidate

* Corresponding author. Mailing address: AIDS Research Center, National Institute of Infectious Diseases, Shinjuku-ku, Tokyo 162-8640, Japan. Phone: 81-3-5285-1111, ext. 2737. Fax: 81-3-5285-1183. E-mail: someyan@nih.go.jp.

HIV-1 vaccine (1, 49), including the ability to induce long-lasting immune responses (7). It is generally accepted that a candidate vaccine against HIV-1 must also be easily administered and affordable in developing countries, and it must be compatible with other commonly administered vaccines (35). If effective, a BCG-based recombinant HIV-1 (rBCG–HIV-1) vaccine would fulfill many of these critical requirements.

Results using other vaccine modalities, in particular, live attenuated SIV vaccines, have raised concerns about the potential for reversion to pathogenicity (3, 4), suggesting that many SIV strains may be potentially virulent. In this study, we used two distinct strains of challenge virus: SHIV-MN (29), which contains V3 sequences homologous to rBCG Env V3, and SHIV-89.6PD (12, 20, 28, 41), which is heterologous in the V3 region and highly pathogenic. We examined whether vaccination with rBCG Env V3 could effectively elicit NAb responses in rhesus macaques and whether it might effectively induce protective immunity against challenge with either SHIV-MN or SHIV-89.6PD.

MATERIALS AND METHODS

Animals. The macaques (*Macaca mulatta*) used in this study originated from China and were purchased through Japan SLC Ltd., Shizuoka, Japan. The animals were maintained according to standard operating procedures established for the evaluation of human vaccines at the Tsukuba Primate Center, National Institute of Infectious Diseases, Tsukuba, Ibaragi, Japan. The study was conducted in the P3 facility for monkeys in the Murayama Branch, National Institute of Infectious Diseases, Musashimurayama, Tokyo, Japan, and in accordance with requirements specified in the laboratory biosafety manual of the World Health Organization.

Construction of the rBCG Env V3 immunogen. rBCG substrain Tokyo was produced by transfection of BCG-Tokyo 172 cells with plasmid pSO246 as described previously (21, 22, 30). The XhoI site of this plasmid was used to insert a mycobacterial codon-optimized DNA fragment encoding 19 amino acids of the Japanese HIV-1 V3 consensus sequence (NTRKSIHIGPGRAFYATGS), which has a neutralization sequence identical to that of HIV-1_{MN} (16, 23, 39, 52). The resulting rBCG vector was designated rBCG Env V3. By semiquantitation of a chimeric protein consisting of the V3 peptides and α-K protein (9), the concentration of the secreted protein was estimated to range from 1 to 3 μg/ml in the culture filtrate of rBCG Env V3 (data not shown).

Viruses. Viruses used in challenge experiments were kindly provided by Y. Lu, Harvard AIDS Institute, Cambridge, Mass. The SHIV-MN virus stock was prepared in concanavalin A-activated macaque peripheral blood mononuclear cells (PBMC) from normal animals, and the amount of virus was quantified by SIV p27 antigen enzyme-linked immunosorbent assay (ELISA) (Coulter Co., Hialeah, Fla.). The tissue culture infective dose (TCID) of the stock was measured on CEMx174 cells (AIDS Research and Reference Reagent Program, National Institutes of Health, Rockville, Md.). Stocks of HIV-1_{MN} and HIV-1_{IIIB} (AIDS Research and Reference Reagent Program) were prepared by propagating 100 50% TCID ($TCID_{50}$) of each virus in phytohemagglutinin-activated normal human PBMC, as described previously (17). The primary isolate, HIV-1_{MNp}, was kindly provided by J. Sullivan, University of Massachusetts Medical School, Worcester, Mass. All other viruses were obtained from the AIDS Research and Reference Reagent Program. Cell-free virus stocks were stored at −130°C until they were used.

V3-specific ELISA. HIV-1 V3 peptide-based ELISAs were used for titration and quantification of serum antibodies for detection as described previously (14). In brief, 96-well ELISA plates (MaxiSorp; Nunc A/S, Roskilde, Denmark) were coated with 100 μl of peptide MN (DKRIHIGPGRAFYTT)/well in 50 mM carbonate buffer (pH 9.3) at 5 μg/ml overnight at 4°C. The wells were washed and treated with 5% nonfat milk in phosphate-buffered saline for 1 h at 37°C. Duplicate samples containing either control or test macaque serum at appropriate dilutions were then added at 100 μl/well, and the plates were incubated for 1 h at 37°C. The wells were washed and incubated with a detection antibody solution consisting of peroxidase-conjugated goat anti-monkey immunoglobulin G (IgG) antibody (EY laboratories Inc., San Mateo, Calif.) at 100 μl/well for 1 h at 37°C. After final washes with 0.05% Tween-20–phosphate-buffered saline (PBST), peroxidase substrate was added, and the reaction was stopped by the addition of 0.5 M H_2SO_4.

IFN-γ ELISPOT assay. Enzyme-linked immunospot (ELISPOT) assays were performed using the method developed by Mothe and Watkins of the Wisconsin University Primate Center and described elsewhere (18, 33). In brief, 96-well flat-bottom plates (U-CyTech-BV, Utrecht, The Netherlands) were coated with anti-gamma interferon (IFN-γ) monoclonal antibody before being washed with PBST and blocked with bovine serum albumin. Freshly isolated PBMC were mixed with either concanavalin A or 2 μM V3 peptide and were then incubated for 16 h at 37°C in 5% CO_2 in anti-IFN-γ-coated plates. Once the plates had been washed, rabbit anti-IFN-γ polyclonal biotinylated detector antibodies were added, and the plates were incubated. Gold-labeled anti-biotin IgG solution (U-CyTech-BV) was added to the plates after they were washed with PBST. The plates were then incubated for 1 h at 37°C. Developed wells were imaged, and spot-forming cells (SFC) were counted using the KS ELISPOT compact system (Carl Zeiss, Oberkochen, Germany). An SFC was defined as a large black spot with a fuzzy border (33).

In vitro virus neutralization assays. GHOST cell neutralization assays were performed as previously described (8). Briefly, GHOST cells expressing either CXCR4 or CCR5 were used as targets for HIV-1 infection (50, 54). The cells were analyzed by FACSCalibur flow cytometry (Becton Dickinson, San Jose, Calif.), and 15,000 events were scored. The mean number of fluorescent GHOST cells determined from negative controls plus 2 standard deviations was considered the cutoff for a positive sample. Purified human immunoglobulin (Nihon Pharmaceutical Co., Tokyo, Japan) and saline were included as additional controls.

M8166 cell-based virus neutralization assays were also performed as described previously (16, 47). In brief, the in vitro neutralization activity of purified macaque IgG was determined using 100 $TCID_{50}$ of either HIV-1_{MN} or SHIV-MN in cultures of M8166 cells. The results were compared with parallel cultures to which preimmune serum IgG was added. Neutralization was expressed as percent inhibition of HIV-1 p24 or SIV p27 antigen production in the culture supernatants. Purified normal macaque IgG was used as a control.

Quantification of cell-associated viral load. Levels of cell-associated virus were quantified by limiting dilution of PBMC (from 10^6 to 1 cells), and the virus was cocultured with M8166 cells as described previously (17). Virus released into the culture supernatant was measured by SIV p27 antigen ELISA (Coulter). The smallest number of PBMC required to produce a positive culture was considered the end point, and the titer of infectious virus was expressed as $TCID_{50}$ per 10^6 PBMC.

PCR detection of proviral HIV-1 infection of rhesus macaques. PBMC with SHIV were detected by DNA PCR using a primer pair that spans the C2-V3 sequence of HIV-1_{IIIB}, followed by Southern blotting with an SE1 probe, 5′-GCAGAAGAAGAGGTAGTAATTAGAT-3′ (nucleotides 7019 to 7043) (47). The positions of the oligonucleotides are numbered relative to the HIV-1_{HXB2} isolate in the ENTREZ database (National Center for Biotechnology Information, National Library of Medicine, National Institutes of Health, Bethesda, Md.). Viral DNA was quantified by comparison with standards derived from 8E5/LAV cells, which contain one copy of HIV-1 proviral DNA per cell (AIDS Research and Reference Reagent Program).

Competitive PCR quantitation of SHIV RNA in plasma. Quantitative, competitive reverse transcription-PCR was performed using a competitor RNA and a DNA template as previously described (18, 32, 44). The detection limit of this assay was 500 RNA copies/ml in monkey plasma (18, 32).

Sequencing of HIV-1 Env C2-V3 sequence. To determine the sequence of the HIV-1 Env C2-V3 region, mRNA was extracted from stock virus and cDNA was synthesized using a Micro-FastTrack version 2.0 kit (Invitrogen, Carlsbad, Calif.) and a cDNA cycle kit (Invitrogen) according to the manufacturer's instructions. The PCR products were cloned into a pCR II vector with a dual promoter using a TA cloning kit (Invitrogen) (47). Sequence analysis was performed using a Big Dye terminator cycle-sequencing FS kit (Perkin-Elmer, Foster City, Calif.) and automated ABI 310 sequencer (Perkin-Elmer) with Sp6 and T7 sequence primers (Invitrogen). Sequence data were compared with published HIV-1 sequences in GenBank (National Center for Biotechnology Information, National Institutes of Health).

Statistical analysis. Calculations of the geometric mean ± standard deviation (SD) were carried out with a microcomputer. Significance was defined as a P value of <0.05.

RESULTS

Vaccination protocol. Twenty-four male rhesus macaques (R-01 through R-24) were enrolled in the study. Of these, 15 were subcutaneously immunized for 24 weeks with 10 mg of

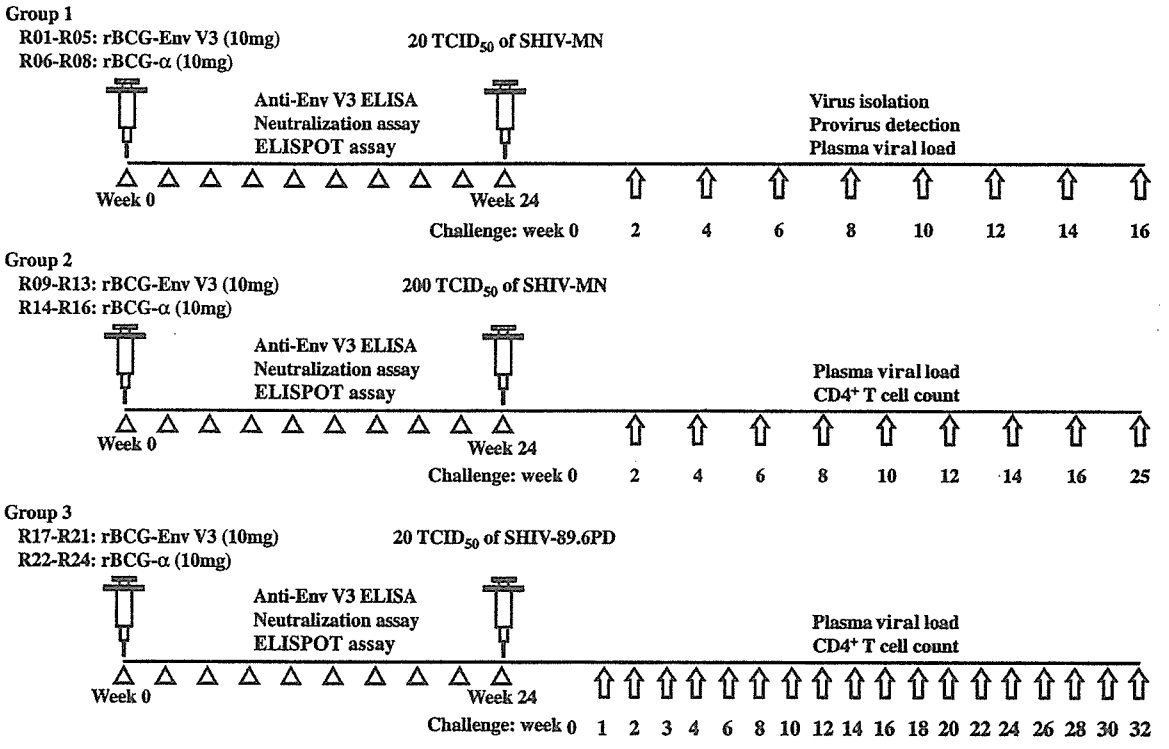

FIG. 1. Schematic representation of the experimental protocol for immunization of rhesus macaques with rBCG Env V3 and challenge with either SHIV-MN or SHIV-89.6PD. A total of 24 macaques were assigned to either the rBCG Env V3 vaccine or rBCG vector control group. The animals each received a single subcutaneous injection and were then split into three groups prior to challenge with either low-dose SHIV-MN, high-dose SHIV-MN, or SHIV-98.6PD.

rBCG Env V3 (16), which expresses and secretes a chimeric protein consisting of α-antigen and the Env V3 region of HIV-1_{MN}. The remaining nine macaques were immunized by the same route and with the same dose of rBCG α-antigen and served as vector controls. All macaques inoculated with rBCG Env V3 remained in good health following vaccination. Three of the 15 immunized macaques experienced transient redness with slight erosion localized at the injection site; however, the reaction spontaneously resolved within 3 months. Following immunization, the 24 macaques were divided into three groups, each group consisting of five immunized animals and three vector controls. The macaques within each group received an intravenous challenge with either SHIV-MN (20 or 200 $TCID_{50}$) or SHIV-89.6PD (20 $TCID_{50}$) (Fig. 1).

Vaccine-induced HIV-specific immune responses following rBCG Env V3 immunization. (i) Neutralizing antibodies. As described above, 15 rhesus macaques were vaccinated with a single subcutaneous inoculation of 10 mg of rBCG Env V3. Induction of HIV-1-specific immunity was measured 24 weeks later in blood samples obtained pre- and postvaccination. All 15 immunized macaques exhibited HIV-1 Env V3 peptide-binding antibody activity by ELISA at serum dilutions ranging from 1:640 to 1:10,240 (Fig. 2). Antibody responses were monophasic, peaking at 4 to 6 weeks and then gradually declining. Serum samples obtained from naïve macaques were consistently negative by ELISA, while postvaccination sera did not react with a control fusion peptide of HIV gp41 (data not shown).

Antibodies were purified from the macaque sera to remove factors that might interfere with certain bioassays (51). The purified antibodies were then tested in vitro for the ability to neutralize SHIV-MN infection in M1866 cells (Fig. 3). Antibodies induced in macaques vaccinated with rBCG Env V3 strongly neutralized both the challenge SHIV-MN (grown in rhesus PBMC) and a T-cell line-adapted (TCLA) laboratory strain, HIV-1_{MN}. A mean 50% inhibitory concentration (IC_{50}) of 0.05 to 0.5 μg of IgG/ml was measured against SHIV-MN, and a mean IC_{90} of ~3.0 μg of IgG/ml was observed against HIV-1_{MN}. Neutralizing activity was detected in serum samples obtained 4 to 6 weeks after vaccination and was maintained for at least 24 weeks. Preimmune serum IgG from nine macaques immunized with vector alone, and IgG from three additional naive macaques (data not shown), did not neutralize either virus.

(ii) Neutralization responses against primary HIV-1 isolates. To further assess the specificity of antibodies in immune sera, neutralizing activity was evaluated against a panel of seven primary HIV-1 isolates using GHOST cells expressing either CCR5 or CXCR4 (Table 1). Purified IgG from macaques in each of the three immunization groups was able to effectively neutralize HIV-$1_{BZ167/X4}$, HIV-$1_{SF2/X4}$, and HIV-$1_{CI2/X4}$ (Table 1 and Fig. 4), with mean IC_{50} values of 5 to 7, 4 to 7, and 5 to 15 μg/ml, respectively. By comparison, neutralization of HIV-$1_{MNp/X4}$ required ~10-fold more serum IgG, with a mean IC_{50} of 50 μg/ml. Three additional isolates, HIV-$1_{SF33/X4}$, HIV-$1_{SF33/R5}$, and the clade A isolate HIV-$1_{VI313/R5}$,

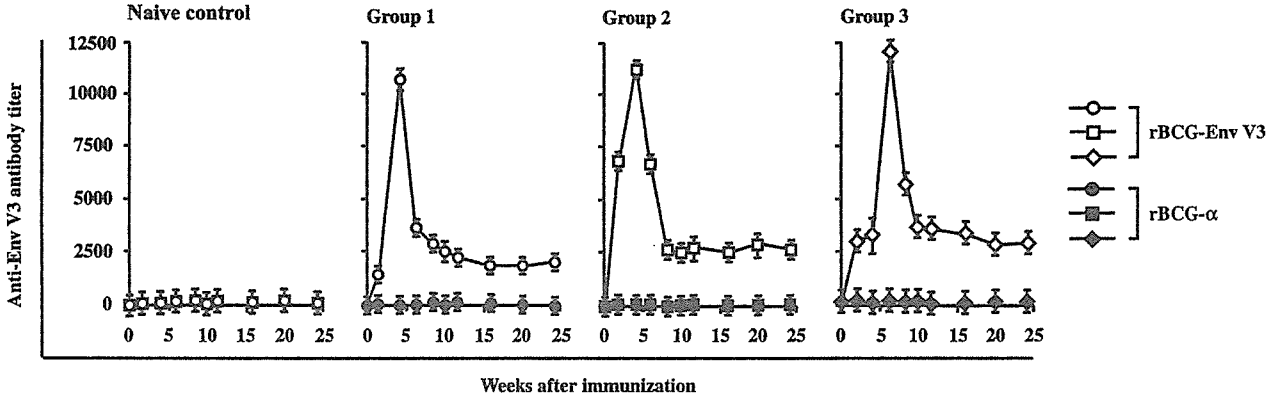

FIG. 2. Serum anti-V3 antibody titers determined by peptide-based ELISA. Preimmune and immune sera from macaques inoculated with rBCG Env V3 were collected and stored at −80°C until they were used. Sera from naïve macaques were used as controls. Data using preimmune sera were within the control levels (data not shown). The results are expressed as the means ± SD of four independent assays.

were not neutralized with serum IgG concentrations up to 50 μg/ml (Table 1). Preimmune sera had no neutralizing activity against any of the isolates. Thus, antibodies present in sera from the immunized macaques were able to neutralize primary HIV-1 isolates, including HIV-1_{BZ167}, HIV-1_{SF2}, and HIV-1_{CI2}, in assays using GHOST cells that express CXCR4 with 10- to 50-fold-higher sensitivity than that of the dual-tropic (X4-R5) TCLA strain HIV-1_{MNp}. Among the neutralization-sensitive viruses, the V3 sequence motifs of HIV-1_{BZ167} and HIV-1_{SF2} shown in Fig. 5 did not correlate with the observed neutralization profiles of HIV-1 Env V3.

(iii) V3 peptide-specific T-cell responses. Table 2 offers a comparison of the virus-specific T-cell response levels determined by IFN-γ ELISPOT analysis in immunized animals with the neutralization data provided in Fig. 2. Of the 15 animals immunized with rBCG Env V3 (180 and 160 SFC/10^6 PBMC at 6 weeks postimmunization [p.i.], respectively), only R-09 and R-10 showed very low levels of SFC activities at the time of

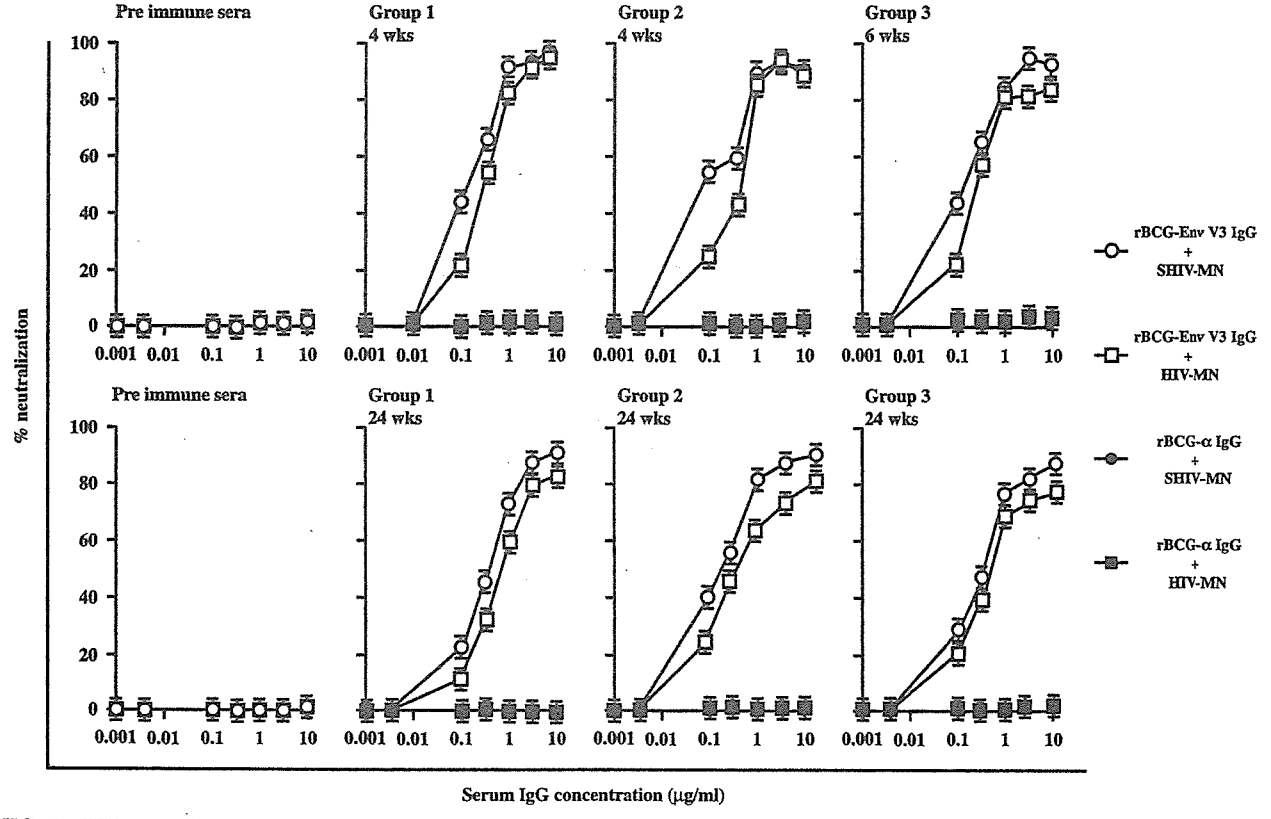

FIG. 3. HIV-1-specific neutralization antibody responses in macaques vaccinated with rBCG Env V3. Analysis of in vitro neutralization of SHIV-MN by anti-rBCG-HIV-1 antibodies using M8166 cell-based virus neutralization assays. Serum IgG was purified from preimmune or immune sera of macaques inoculated with rBCG Env V3 at the indicated times. The results are expressed as the means ± SD of four independent assays.

TABLE 1. 50% neutralization calculated on the basis of neutralization curves[a]

Serum sample	Neutralizing activity (μg)						
	BZ167/X4	MNp/X4	SF2/X4	SF33/X4	SF33/R5	V1313/R5	C12/X4
Group 1	6.5	50	7	>50	>50	>50	10
Group 2	5	50	4	>50	>50	>50	5
Group 3	7	50	6.5	>50	>50	>50	15
Pre immunization sera of groups 1, 2, and 3	>50	>50	>50	>50	>50	>50	>50

[a] The neutralization assays with the various viruses were carried out in GHOST cells expressing either CXCR4 (X4) or CCR5 (R5) as indicated in Fig. 4. BZ167, MNp, SF2, SF33, and CI-2 are HIV-1 clade B viruses. VI313 is an HIV-1 clade A virus.

SHIV challenge (120 and 110 SFC/10^6 PBMC at 24 weeks p.i., respectively) (Table 2). In contrast, <100 SFC/10^6 PBMC were observed in other immunized animals, and <20 SFC/10^6 PBMC were observed in controls. Thus, the V3 region antigen in the rBCG Env V3 proved unable to induce significant levels of virus-specific T-cell responses in immunized animals.

Challenge with low-dose SHIV-MN. The first group of eight macaques (R-01 through R-08), consisting of five animals that received rBCG Env V3 and three that received control rBCG α-antigen, were intravenously challenged with low-dose SHIV-MN (20 $TCID_{50}$) at 24 weeks p.i. The cell-associated virus load was measured in PBMC cocultures, and proviral copy numbers were estimated by DNA PCR using primary PBMC genomic DNA. The level of plasma viremia in each macaque was quantified by competitive reverse transcription-PCR to assess infection and virus replication for 16 weeks after virus challenge (Table 3).

Control macaques vaccinated with the vector alone (R-06 through R-08) were positive in all three viral-load assays 2 weeks after SHIV-MN challenge and remained positive for a follow-up period of 10 weeks. Because only low levels of viral RNA (<10^4 RNA copies/ml) were transiently detected 2 weeks postchallenge, all three assays (virus isolation, plasma RNA, and proviral DNA) were used for virus detection. Using these criteria, we observed that all three parameters remained negative after low-dose SHIV-MN challenge in three of five macaques vaccinated with rBCG Env V3 (R-02, R-04, and R-05). However, macaque R-01 was transiently positive in all three assays for virus infection at 4 weeks. Another macaque immunized with rBCG Env V3 (R-03) exhibited a sharp in-

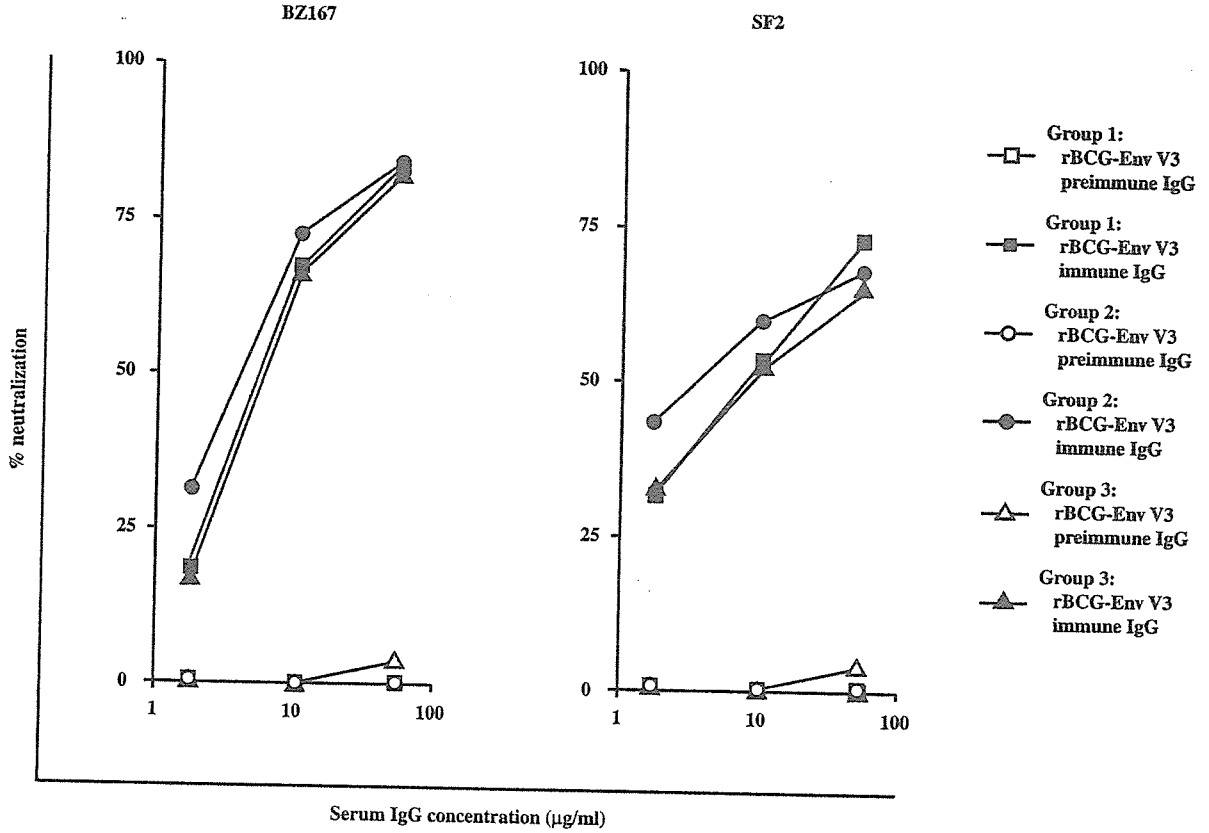

FIG. 4. Neutralization of HIV-1_{BZ167} and HIV-1_{SF2} in GHOST-X4 cells by immune sera from macaques vaccinated with rBCG Env V3. Dilutions of immune sera (closed symbols) and preimmune sera (open symbols) were tested in duplicate, and the percent neutralization was calculated using the mean value. The dose-response curves represent the means of three independent assays.

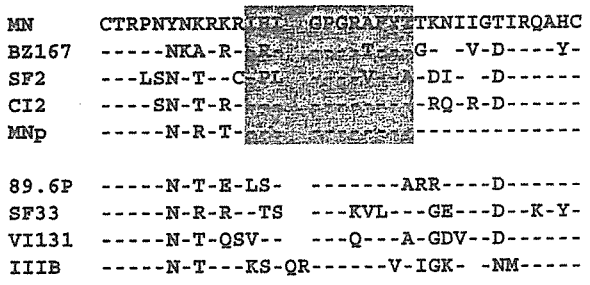

FIG. 5. Alignment of the amino acid sequences of HIV-1 Env V3 from primary and laboratory isolates. The spaces indicate amino acid deletions; dashes indicate homology. The V3 motif of a neutralization-sensitive HIV-1 strain is enclosed in the shaded rectangle (37).

crease in viral load following challenge, and the levels remained high until the animal was sacrificed. These results demonstrate that vaccination with rBCG Env V3 can induce protective immunity in rhesus macaques against a low-dose challenge with SHIV-MN.

Challenge with high-dose SHIV-MN. The second group of eight macaques (R-09 through R-16) was similarly challenged with a higher dose (200 $TCID_{50}$) of SHIV-MN by intravenous inoculation at 24 weeks p.i. (Fig. 6). Measurements of the viral loads in PBMC and plasma indicated that all the macaques were infected by the high-dose SHIV-MN challenge. However, the level of viremia during the acute phase of viral infection was reduced by 1 to 2 log units in macaques immunized with rBCG Env V3 compared with controls (from 10^6 to 10^7, to $<10^5$ to 10^4 RNA copies/ml) (Fig. 6A). The control macaques developed a transient decrease in $CD4^+$-T-cell counts that rebounded to normal levels ~3 weeks postchallenge (Fig. 6B). In contrast, macaques vaccinated with rBCG Env V3 had little or no change in $CD4^+$-T-cell numbers.

Despite the low levels of V3 peptide-specific IFN-γ ELISPOT activities noted for animals R-09 and R-10 above (Table 2), these animals exhibited a plasma viral load and a rate of $CD4^+$-cell loss after SHIV challenge that was comparable to those seen in the immunized animals designated R-11, -12, and -13. Thus, immunization with rBCG Env V3 generated even low levels of T-cell responses in only 2 animals out of 5 in this group and out of a total of 15 immunized animals. No evidence of higher virus-specific IFN-γ ELISPOT activity was demonstrated in samples obtained 0, 4, or 6 and 24 weeks after vaccination (Table 2), suggesting that few significant cellular anti-SHIV responses were generated and that those few did not affect virus control in this macaque population.

Challenge with pathogenic SHIV-89.6PD. The third group of macaques (R-17 through R-24) was challenged with pathogenic SHIV-89.6PD (20 $TCID_{50}$) 24 weeks postinoculation. The effects of vaccination with rBCG Env V3 on immune induction against the pathogenic virus were followed for 32 weeks, and the macaques were then autopsied. As shown in

TABLE 2. SHIV-MN-specific serum IgG neutralization titers and Env V3-specific ELISPOT responses[a]

Monkey no.	Immunogen	IC_{50} of neutralization serum IgG (μg/ml)[b]			V3-specific IFN-γ SFCs/10^6 cells[c]		
		0 week	4 or 6 weeks[d]	24 weeks[e]	0 week	4 or 6 weeks	24 weeks
R-01	rBCG Env V3	>50	0.5	0.6	<20	30	20
R-02	rBCG Env V3	>50	0.3	0.4	<20	40	40
R-03	rBCG Env V3	>50	0.5	0.6	<20	40	30
R-04	rBCG-Env V3	>50	0.2	0.3	<20	20	40
R-05	rBCG-Env V3	>50	0.08	0.3	<20	30	80
R-06	rBCG-α	>50	>50	>50	<20	<20	<20
R-07	rBCG-α	>50	>50	>50	<20	<20	<20
R-08	rBCG-α	>50	>50	>50	<20	<20	<20
R-09	rBCG-Env V3	>50	0.04	0.3	<20	180	120
R-10	rBCG-Env V3	>50	0.1	0.2	<20	160	110
R-11	rBCG-Env V3	>50	0.05	0.2	<20	20	30
R-12	rBCG-Env V3	>50	0.03	0.4	<20	60	20
R-13	rBCG-Env V3	>50	0.02	0.4	<20	30	30
R-14	rBCG-α	>50	>50	>50	<20	<20	<20
R-15	rBCG-α	>50	>50	>50	<20	<20	<20
R-16	rBCG-α	>50	>50	>50	<20	<20	<20
R-17	rBCG-Env V3	>50	0.2	0.6	<20	40	90
R-18	rBCG-Env V3	>50	0.3	0.3	<20	50	60
R-19	rBCG-Env V3	>50	0.3	0.4	<20	40	30
R-20	rBCG-Env V3	>50	0.5	0.7	<20	20	50
R-21	rBCG-Env V3	>50	0.4	0.5	<20	20	40
R-22	rBCG-α	>50	>50	>50	<20	<20	<20
R-23	rBCG-α	>50	>50	>50	<20	<20	<20
R-24	rBCG-α	>50	>50	>50	<20	<20	<20

[a] Animals were inoculated with either rBCG Env V3 or the vector control. Blood samples were obtained at 0, 4, or 6 and 24 weeks p.i., and antibody inhibitory concentration and the V3-specific IFN-γ ELISPOT activity were compared.
[b] The IC_{50} was derived from the data in Fig. 2 based on neutralization dose-response curves similarly obtained from Fig. 3.
[c] Freshly isolated PBMC were assessed for their ability to produce IFN-γ in response to HIV-1_{MN} Env V3 peptide.
[d] Mean IC_{50}s: R-01 to R-05, 0.32; R-09 to R-13, 0.05; R-17 to R-21, 0.35.
[e] Mean IC_{50}s: R-01 to R-05, 0.44; R-09 to R-13, 0.30; R-17 to R-21, 0.50.

TABLE 3. Comparison of low-dose SHIV-MN infections in macaques vaccinated with either rBCG Env V3 or rBCG-α (control)

Monkey	Immunogen (10 mg)	Efficacy analysis	Results[a]							
			0[b]	2	4	6	8	10	12	16
R-01	rBCG Env V3	Virus isolation	<1	<1	2	<1	<1	<1	<1	<1
		Provirus by PCR	<500	<500	>500	<500	<500	<500	<500	<500
		Plasma viral load	<500	<500	20,000	<500	<500	<500	<500	<500
R-02	rBCG Env V3	Virus isolation	<1	<1	<1	<1	<1	<1	<1	<1
		Provirus by PCR	<500	<500	<500	<500	<500	<500	<500	<500
		Plasma viral load	<500	<500	<500	<500	<500	<500	<500	<500
R-03	rBCG Env V3	Virus isolation	<1	32	<1	<1	2	<1	ND	ND
		Provirus by PCR	<500	>500	<500	<500	>500	<500	ND	ND
		Plasma viral load	<500	310,000	<500	<500	20,000	<500	ND	<500
R-04	rBCG Env V3	Virus isolation	<1	<1	<1	<1	<1	<1	ND	ND
		Provirus by PCR	<500	<500	<500	<500	<500	<500	ND	ND
		Plasma viral load	<500	<500	<500	<500	<500	<500	<500	<500
R-05	rBCG Env V3	Virus isolation	<1	<1	<1	<1	<1	<1	<1	ND
		Provirus by PCR	<500	<500	<500	<500	<500	<500	<500	ND
		Plasma viral load	<500	<500	<500	<500	<500	<500	<500	<500
R-06	rBCG-α	Virus isolation	<1	32	16	<1	2	2	<1	1<
		Provirus by PCR	<500	>500	>500	>500	>500	>500	>500	500
		Plasma viral load	<500	300,000	50,000	20,000	20,000	20,000	20,000	20,000
R-07	rBCG-α	Virus isolation	<1	2	32	<1	<1	<1	<1	ND
		Provirus by PCR	<500	>500	>500	>500	>500	<500	<500	ND
		Plasma viral load	<500	27,000	310,000	350,000	25,000	<500	<500	<500
R-08	rBCG-α	Virus isolation	<1	32	16	<1	2	2	ND	ND
		Provirus by PCR	<500	>500	>500	>500	>500	>500	ND	ND
		Plasma viral load	<500	300,000	50,000	<500	20,000	20,000	ND	<500

[a] Viral loads were determined by either limiting dilution of PBMC or competitive PCR for HIV-1 Env V3 genes, and the results are expressed as the number of infected cells per million PBMC and virus copies per milliliter of blood. Nested PCR for HIV-MN Env V3 was used in all macaques to detect the provirus genome. Naïve macaques were injected intravenously with 20 $TCID_{50}$ of SHIV-MN and used as controls for SHIV infection. The results are expressed as the mean of three different assays; <1, <500, and <500 were the detection limits of virus isolation, proviral copy number, and plasma viral load, respectively. ND, not determined.

[b] Weeks after challenge.

Fig. 7, high levels of plasma viremia were detected in the control macaques, with a viral set point of ~10^6 RNA copies/ml, accompanied by an abrupt decline in $CD4^+$-T-cell counts. Prior vaccination with rBCG Env V3 appeared to have no positive effect on the viral load and $CD4^+$-T-cell counts compared with the control animals.

Association of in vitro neutralization antibody responses following rBCG Env V3 immunization with control of viremia after SHIV challenge. Of the macaques challenged with low doses of homologous SHIV-MN (group 1), the three virus-controlled macaques R-02, -04, and -05 (Table 1) had higher IC_{50}s of SHIV-MN-specific neutralizing antibodies as measured in M8166 cells at 24 weeks p.i. or on the day of challenge, with serum IgG concentrations of 0.4, 0.3, and 0.3 μg/ml, respectively (Table 2). The IC_{50}s of the uncontrolled macaques R-01 and -03 (Table 1) were both 0.6 μg/ml (Table 2).

When the challenge dose was increased 10-fold (Fig. 1), all five animals in group 2 had high neutralizing antibody titers with a mean IC_{50} of 0.30 μg/ml on the day of challenge (Table 2). These animals in group 2 showed partial protection against the same homologous virus challenge (Fig. 6). In contrast, no animals similarly immunized with rBCG elicited any in vivo protection against a low-dose, heterologous viral challenge with SHIV-89.6PD (Table 2 and Fig. 7).

In summary, the rBCG Env V3-elicited NAb response afforded some degree of protection against a homologous viral challenge. However, infection by the heterologous virus SHIV-89.6PD was not controlled by heterologous virus SHIV-MN- or HIV-1_{MN}-specific NAb generated by the recombinant HIV-1_{MN} Env V3-expressed BCG immunization.

DISCUSSION

First, our study demonstrates the potential of anti-Env V3 NAb induced by immunization of rhesus macaques with rBCG Env V3 to afford protection against homologous challenge with SHIV-MN but not against the heterologous SHIV-89.6PD. With the low-dose homologous SHIV-MN challenge (20 $TCID_{50}$), sterile protection was achieved in three of five immunized animals. These findings correlate well with our in vitro neutralization data for these animals. Protected animals showed higher levels of potent neutralization antibodies than did unprotected animals. Macaques serving as vector and naïve controls experienced high levels of replication of the SHIV-MN challenge virus. With a high-dose challenge, rBCG Env V3 vaccination was effective at reducing viremia during acute infection by ~100-fold. The vaccine consisted of an rBCG vector that expresses a chimeric HIV-1 Env V3 region peptide and the α-antigen of *M. bovis*. The kinetics and magnitude of the HIV-1 Env V3-specific antibody responses elicited in macaques were comparable to those observed in our previous studies using guinea pigs vaccinated with rBCG Env V3 (9, 16).

Secondly, the levels of neutralizing antibodies generated after injection with a recombinant BCG vector-based vaccine expressing a chimeric protein of HIV-1 Env V3 peptide and α-antigen protein were maintained for at least 24 weeks p.i. with no diminishment in titer. A plausible explanation for the longevity of the neutralizing antibody titers after rBCG immunization is that the carrier protein, α-antigen (also known as MPT59 or antigen 85B), is derived from mycobacteria and has

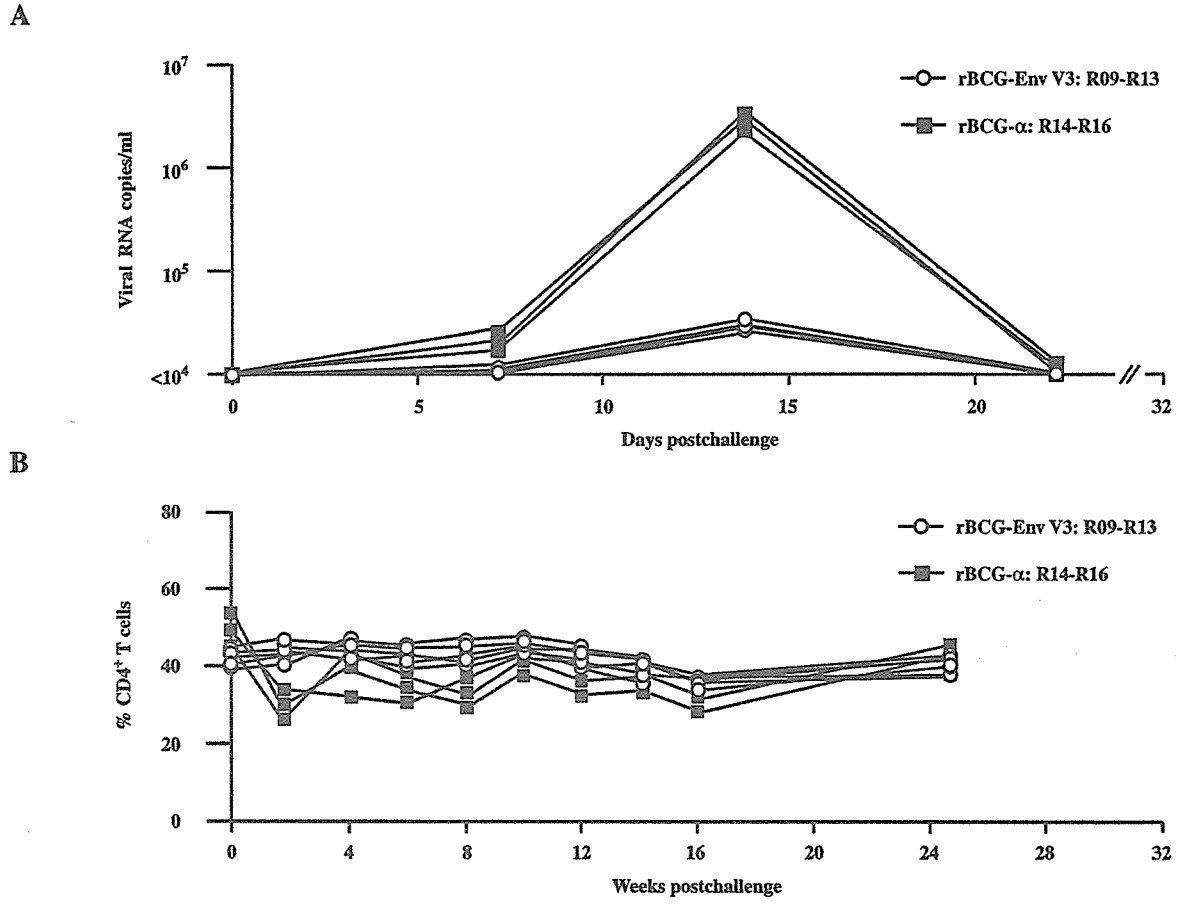

FIG. 6. Comparison of infection kinetics following high-dose (200 $TCID_{50}$) inoculation of SHIV-MN in macaques vaccinated with either rBCG Env V3 or rBCG vector control. (A) Viral RNA copy number per milliliter of serum. (B) $CD4^+$-T-cell count as a percentage of total lymphocytes. The results in individual animals are expressed.

the ability to elicit potent Th1-type immune responses (24, 43). Our result is consistent with those of other groups, which have shown that BCG immunity is maintained for at least a few years and that the BCG bacillus is effective at increasing NAb responses (40). These characteristics might help to explain the long-lasting enhanced levels of NAb elicited by vaccination with rBCG Env V3.

The concentration of purified macaque IgG in serum was determined to be ~10 mg/ml. By this estimation, 0.5 mg corresponds to a serum dilution of 1:1 in virus neutralization assays. The IC_{50} and IC_{90} values for neutralization of SHIV-MN were 10^3 to 10^4 and 166, respectively (similar values were obtained for neutralization of HIV-1_{MN}). These neutralization titers suggest that antibody responses generated de novo may contribute to a degree of protection against SHIV-MN. The observed relationship of the NAb titer and viral protection is consistent with results obtained by repeated immunization with SHIV-89.6 C4-V3 peptides in guinea pigs and rhesus macaques (6, 27). In this case, NAb titers to homologous SHIV-89.6 were ~10^3 greater than those against heterologous HIV-1_{MN}, while responses to HIV-1 R5 viruses were weak or absent. This suggests that the protection mediated by a C4-V3 peptide vaccine against SHIV-89.6 may be type (or strain) specific. Thus, we assume that the NAb generated by SHIV-89.6 C4-V3 peptide immunization (6) would not mediate protection against a heterologous SHIV-MN challenge.

The present study suggests that the vaccine-elicited antibodies directed against the HIV-1 Env V3 peptide can in some cases confer a degree of neutralization against primary isolates of HIV-1 (26). Following vaccination of rhesus macaques with rBCG Env V3, both binding and NAb responses against this novel construct were clearly evident. At the time of SHIV challenge, immune sera from the vaccinated macaques efficiently neutralized a homologous, type-specific TCLA HIV-1 strain (HIV-1_{MN}) and a related SHIV strain (SHIV-MN) with IC_{90} values of <5 μg/ml. Controls, including preimmune sera and sera from macaques vaccinated with rBCG vector alone, had no neutralizing activity in assays using GHOST cells expressing either CCR5 or CXCR4 or in M8166 cells. Immune sera from macaques vaccinated with rBCG Env V3 were able to neutralize several primary HIV-1 X4 isolates (HIV-1_{BZ167}, HIV-1_{SF2}, and HIV-1_{CI2}); however, neutralization of an X4-R5 dual-tropic strain (HIV-1_{MNp}) was weak. No neutralization of HIV-1 R5 isolates and primary HIV-1 isolates from different clades was observed. These findings were confirmed in an independent international neutralization trial (conducted by Simon Beddows and Jonathan Weber, Imperial College School of Medicine, Medical Research Council, London, En-

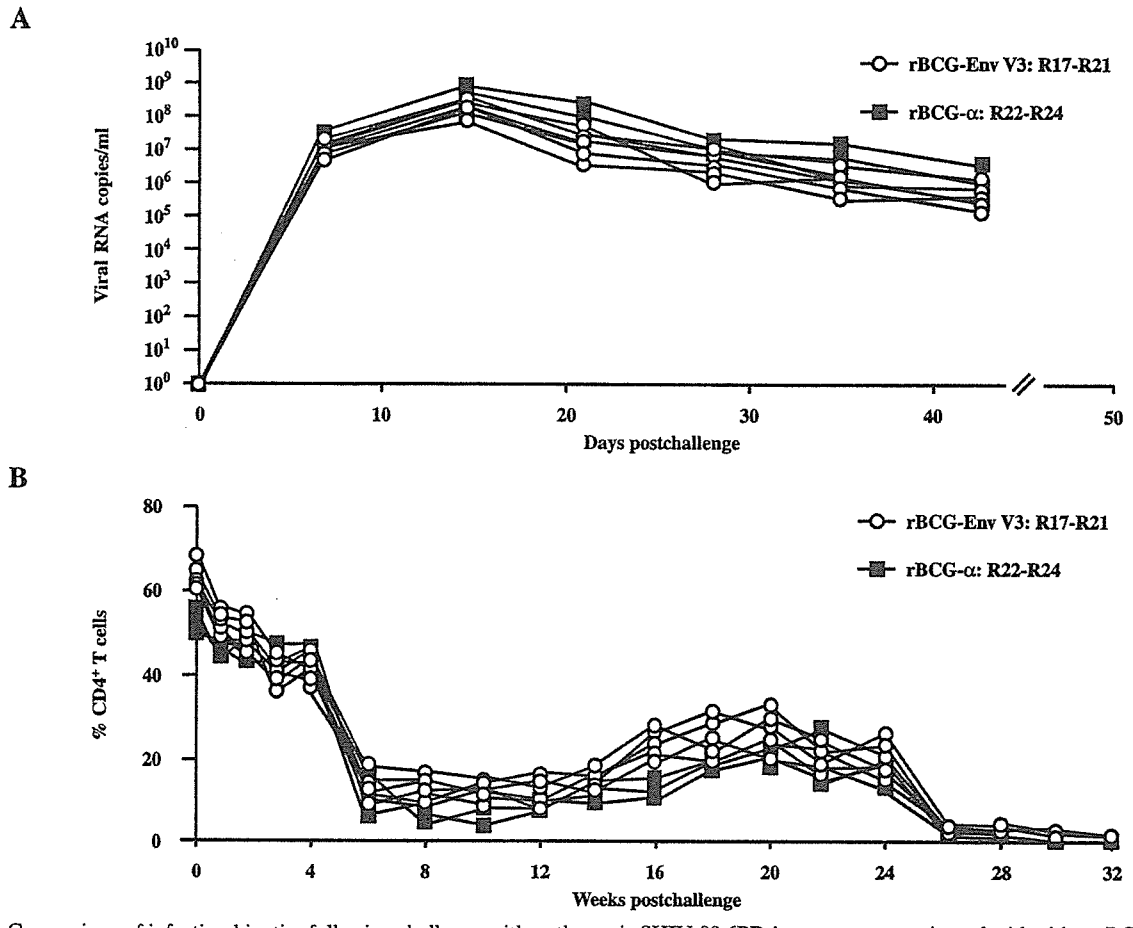

FIG. 7. Comparison of infection kinetics following challenge with pathogenic SHIV-89.6PD in macaques vaccinated with either rBCG Env V3 or rBCG vector control. (A) Plasma viral-RNA copy numbers per milliliter. (B) $CD4^+$-T-cell count as a percentage of total lymphocytes. The results in individual animals are expressed.

gland, and Pia Scott and Eva-Maria Fenyo at Microbiology and Tumorbiology Center, Karolinska Institute, Stockholm, Sweden). Preliminary results from this study have had been summarized and reported (11). Despite similarities in the V3 sequence motif, neutralization of the TCLA strain HIV-1_{MN} was found to be 10- to 50-fold more sensitive than neutralization of primary HIV-1 isolates, such as HIV-1_{CI2}, HIV-1_{MNp}, or HIV-$1_{JR\text{-}CSF}$ (11). A reasonable explanation for the relative insensitivity of primary HIV-1 isolates—particularly primary HIV-1 R5 isolates—to neutralization is the presence of cryptic or occluded sites within the virus-associated V3 region (13, 53).

In the Japanese consensus HIV-1 Env V3 expressed in the rBCG construct, the core V3 motif of the neutralization epitope is IHIGPGRAF (39). Although the consensus sequence of the V3 loop differs from the MN-V3 sequence in five amino acid positions, the neutralization epitope of the tip V3 region in the Japanese consensus is identical to that of MN-V3. Some substitutions of amino acids at certain positions within this motif (for example, H to R and A to T in the core motif in BZ167) are tolerated, suggesting that NAbs generated by immunization with rBCG Env V3 are not strictly type specific. Immune sera from macaques vaccinated with rBCG Env V3 were able to neutralize primary HIV-1 X4 and some HIV-1 X4-R5 dual-tropic isolates, suggesting that the antigenic structure of the chimeric V3 peptide mimics to some extent that of the virus-associated V3 region. Indeed, the chimeric V3–α-antigen protein is estimated to be 38 kDa and contains four cysteine residues, suggesting the possible formation of a new loop structure in the V3 portion of the protein. With regard to the heterologous SHIV-89.6PD challenge in macaques vaccinated with rBCG Env V3, NAbs specific for SHIV-89.6PD were not generated efficiently (IC_{50}, >50 μg of immune serum IgG/ml) and did not provide any protection against the SHIV-89.6PD challenge. The V3 neutralization site of SHIV-89.6PD may differ in sequence or structure or both from that of SHIV-MN or other viral strains, including some of the HIV-1 isolates, making it unrecognizable to antibodies. Such a difference could account for the poor cross-neutralization activity against SHIV-89.6PD.

Thus, our data from the SHIV-macaque models show that the in vitro neutralization titers generated in rBCG-immunized animals correlate with protection. Although a present goal of HIV-1 vaccine development is to reduce the viral set point by eliciting high levels of virus-specific cellular immune responses, induction of cross-reactive NAbs may also contribute to control virus replication in the course of HIV-1 infection and may therefore be useful in the context of a preventive vaccine. Furthermore, although the choice of HIV Env V3 and the